Charmless b decays

Daniel O'Hanlon, *on behalf of the LHCb collaboration*

INFN Bologna

LHCb

Beauty 2019, Ljubljana

Why charmless decays?

- Suppressed in the Standard Model: penguin (loop) and tree diagrams of a similar magnitude

- $b \to s$ and $b \to d$ loop diagrams carry a *different* weak phase to those in the tree diagrams

- Different strong and weak phases can lead to large CP-violation in decay

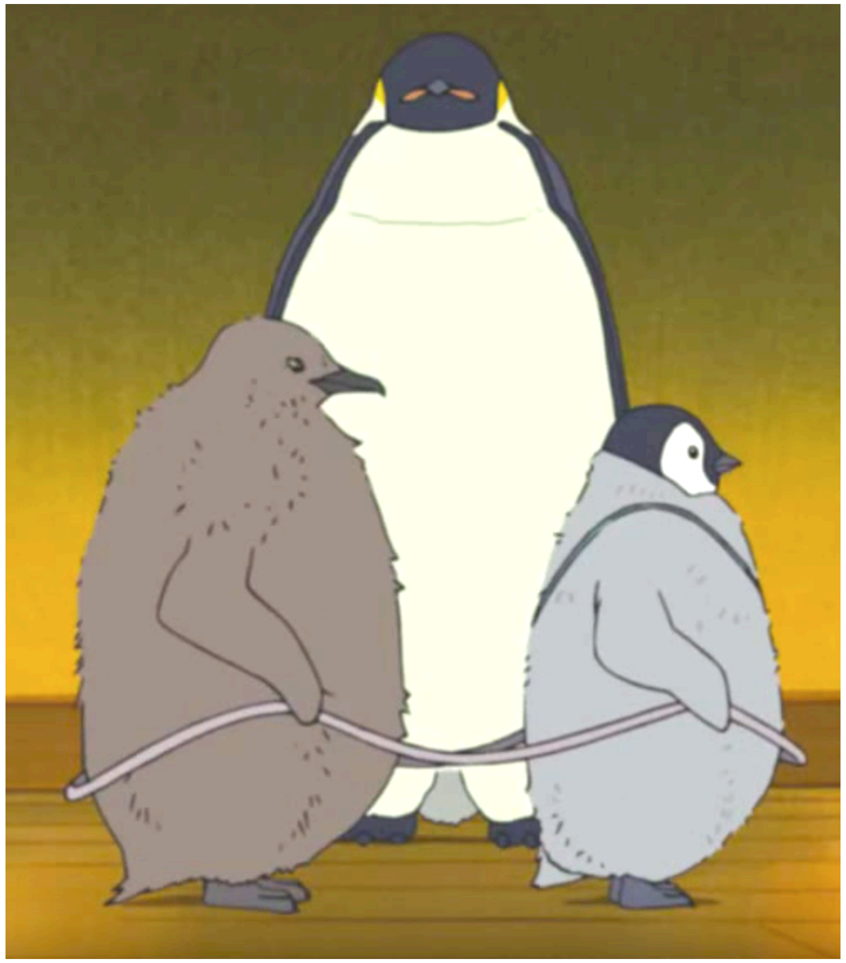

$$\mathcal{A}_{CP} = \frac{\Gamma(\overline{B} \to \overline{f}) - \Gamma(B \to f)}{\Gamma(\overline{B} \to \overline{f}) + \Gamma(B \to f)}$$

$$= \frac{2|A_1||A_2| \sin\delta \sin\phi}{|A_1|^2 + |A_2|^2 + 2|A_1||A_2| \cos\delta \cos\phi},$$

- Inputs to constrain CKM angles, sensitive to new heavy particles off-shell in the loop

Why multibody decays?

- Intermediate resonances and short distance QCD effects result in a strong phase variation across the *Dalitz* plot

→ **CPV in decay!**

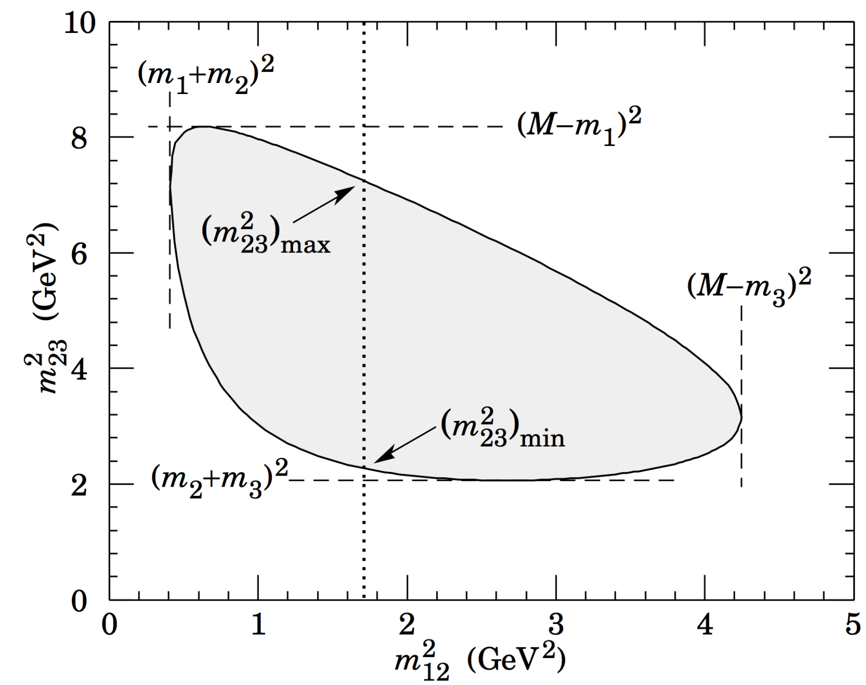

$B^+ \to \pi^+\pi^+\pi^-$ data (Phys. Rev. D 90, 112004 (2014)):

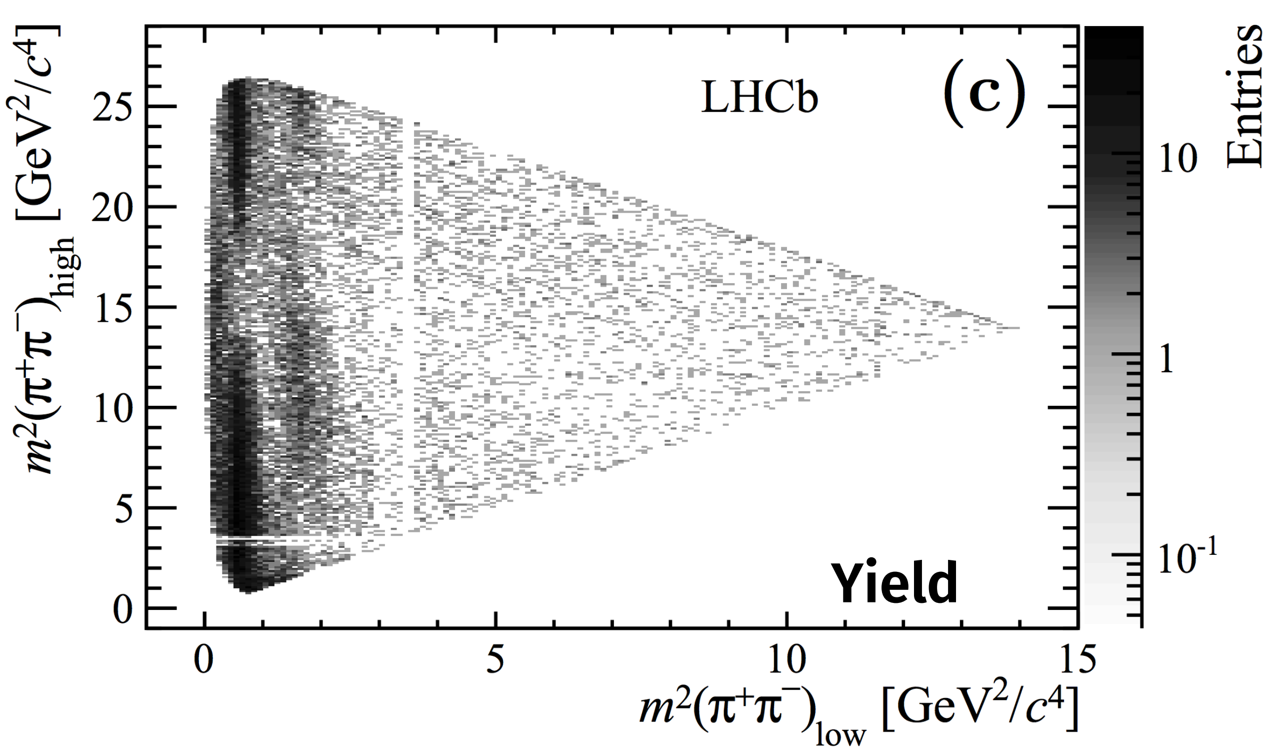

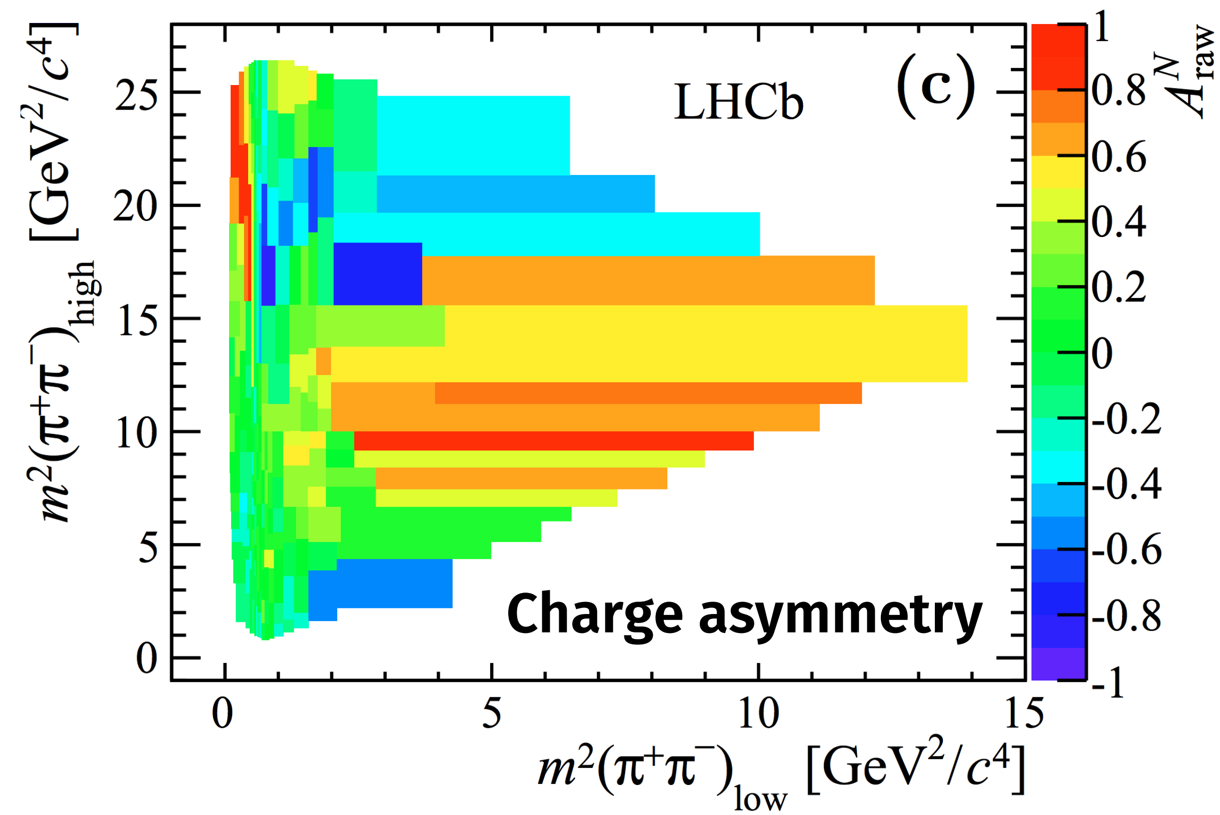

$B^+ \to \pi^+\pi^+\pi^-$

LHCb-PAPER-2019-017
arXiv:1909.05212, Submitted to PRD

LHCb-PAPER-2019-018
arXiv:1909.05211, Submitted to PRL

- **New** analysis (3 fb^{-1} of Run 1 LHCb data):

Construct an explicit **amplitude model** for the decay

- **Three** approaches, that differ in the S-wave (spin-0) description:

'K-matrix':
Single unitarity conserving model, with parameters from scattering data

'Isobar':
Individual hand-engineered components for each contribution, does not conserve unitarity

'Quasi-model-independent':
Fit for a magnitude and phase in bins of the phase-space

The ‘K-matrix’ S-wave model

Sum over resonance poles

arXiv:hep-ph/0204328
(Anisovich & Sarantsev)

Phase space

Production vector

$$\mathcal{F}_u = \sum_{v=1}^{n} [I - i\hat{K}\rho]^{-1}_{uv} \cdot \hat{P}_v \,,$$

Rescattering matrix

Describes initial B ‘production’ state, and propagation into all final states:

$$\hat{K}_{uv}(s) = \left(\sum_{\alpha=1}^{N} \frac{g_u^{(\alpha)} g_v^{(\alpha)}}{m_\alpha^2 - s} + f_{uv}^{\text{scatt}} \frac{m_0^2 - s_0^{\text{scatt}}}{s - s_0^{\text{scatt}}} \right) f_{A0}(s)$$

Parameters from scattering data (fixed)

$$\hat{P}_v(s) = \sum_{\alpha=1}^{N} \frac{\beta_\alpha g_v^{(\alpha)}}{m_\alpha^2 - s} + f_v^{\text{prod}} \frac{m_0^2 - s_0^{\text{prod}}}{s - s_0^{\text{prod}}}$$

Parameters from extracted from fit

The 'K-matrix' S-wave model

Poles

Parameters from scattering data (fixed)

Channels

Couplings

α	m_α	$g_1^{(\alpha)}[\pi\pi]$	$g_2^{(\alpha)}[K\bar{K}]$	$g_3^{(\alpha)}[4\pi]$	$g_4^{(\alpha)}[\eta\eta]$	$g_5^{(\alpha)}[\eta\eta']$
1	0.65100	0.22889	−0.55377	0.00000	−0.39899	−0.34639
2	1.20360	0.94128	0.55095	0.00000	0.39065	0.31503
3	1.55817	0.36856	0.23888	0.55639	0.18340	0.18681
4	1.21000	0.33650	0.40907	0.85679	0.19906	−0.00984
5	1.82206	0.18171	−0.17558	−0.79658	−0.00355	0.22358
	$s_0^{\rm scatt}$	$f_{11}^{\rm scatt}$	$f_{12}^{\rm scatt}$	$f_{13}^{\rm scatt}$	$f_{14}^{\rm scatt}$	$f_{15}^{\rm scatt}$
	−3.92637	0.23399	0.15044	−0.20545	0.32825	0.35412
	$s_0^{\rm prod}$	m_0^2	s_A	s_{A0}		
	−3.0	1.0	1.0	−0.15		

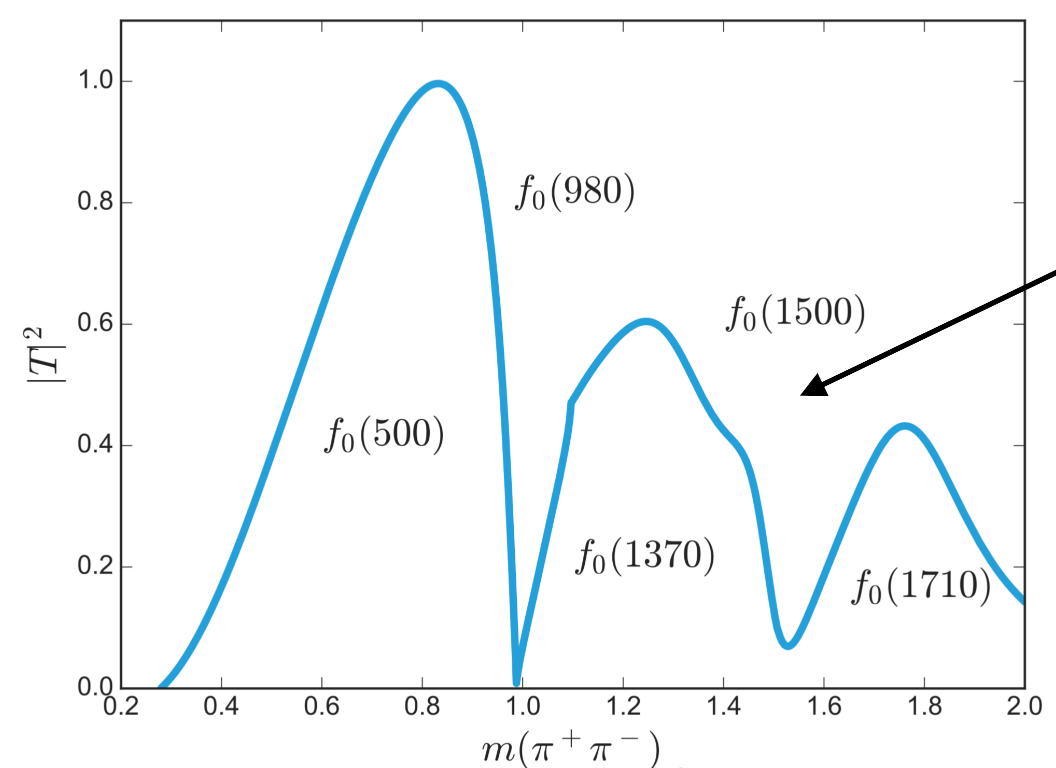

Describes entire S-wave in a single model

The 'Isobar' S-wave model

Simple pole, plus a 'rescattering' term:

Phys. Rev. D 92, 054010 (2015), Phys. Rev. D 89, 094013 (2014)

$$A_{\text{source}}(m) = [1 + (m/\Delta^2_{\pi\pi})]^{-1}[1 + (m/\Delta^2_{KK})]^{-1}$$

$$A_{\text{scatt}}(m) = A_{\text{source}}(m)\, f_{\text{rescatt}}(m).$$

$$f_{\text{rescatt}}(m) = \sqrt{1 - \eta(m)^2}e^{2i\delta(m)}$$

Phase

$$\cot\delta = c_0 \frac{(s - M_s^2)(M_f^2 - s)}{M_f^2 s^{1/2}} \frac{|k_2|}{k_2^2},$$

Inelasticity

$$\eta = 1 - \left(\epsilon_1 \frac{k_2}{s^{1/2}} + \epsilon_2 \frac{k_2^2}{s}\right) \frac{M'^2 - s}{s}$$

$$k_2 = \frac{\sqrt{s - 4m_K^2}}{2};$$

Parameters from $\pi\pi \to \pi\pi$ and $\pi\pi \to KK$ scattering data

Phys.Rev. D71 (2005) 074016

The ‘QMI’ S-wave model

- 17 bins - 14 below the charm veto, 3 above

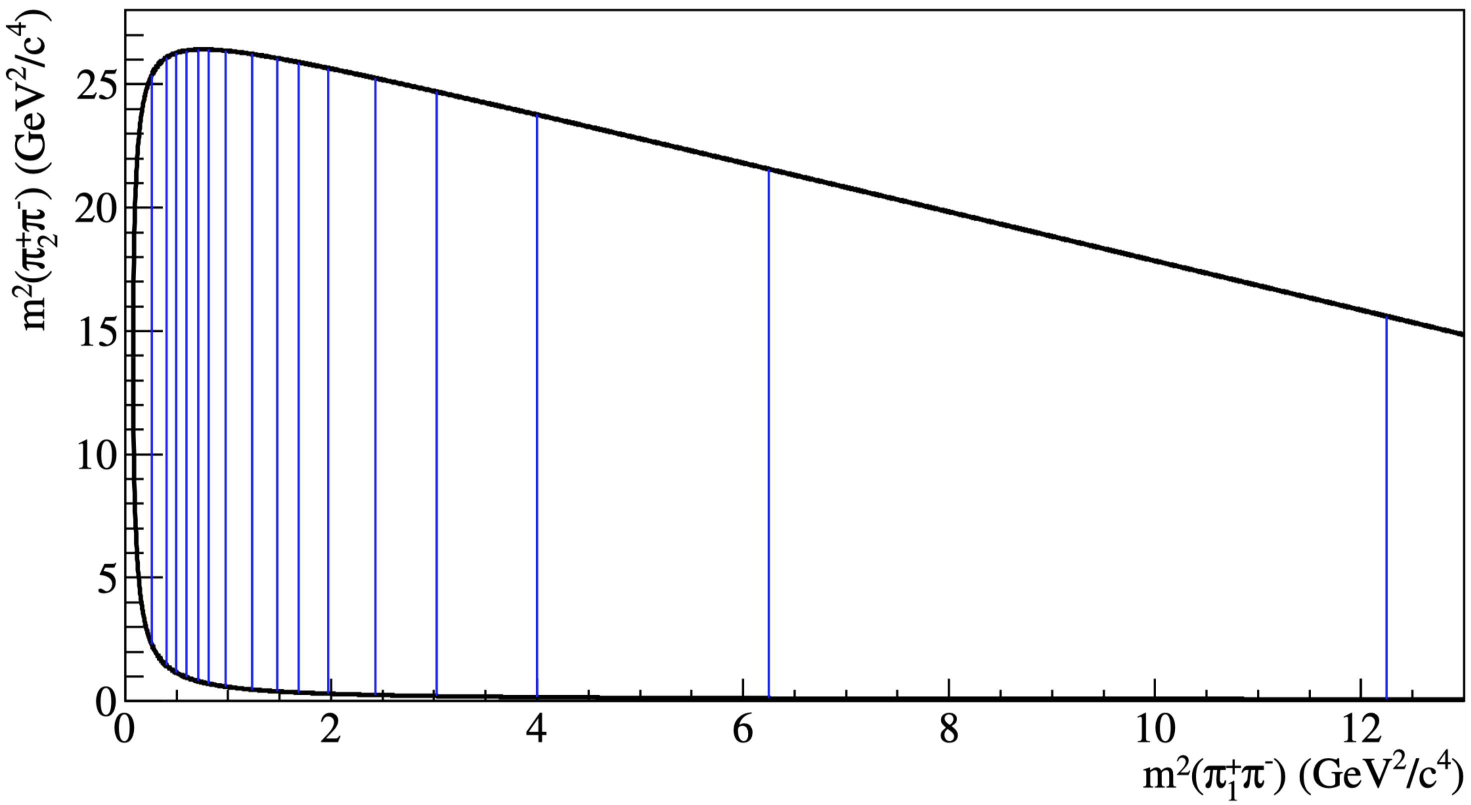

- Fit an independent magnitude and phase in each bin

Model construction

- Start with components identified by the BaBar analysis of this mode, that used 20x fewer signal candidates **Phys. Rev. D72 (2005) 052002**
- Include additional components based on a **likelihood ratio test**, with a threshold of 10 units of negative log-likelihood for inclusion

S-wave	(See previous slide)
$\rho(770)^0$	**Gounaris-Sakurai model**
$\omega(782)$	Relativistic Breit-Wigner
$f_2(1270)$	Relativistic Breit-Wigner
$\rho(1450)^0$	Relativistic Breit-Wigner
$\rho_3(1690)^0$	Relativistic Breit-Wigner

More accurate model for $\rho(770)^0$ width

$B^+ \to \pi^+\pi^+\pi^-$

LHCb-PAPER-2019-017
LHCb-PAPER-2019-018

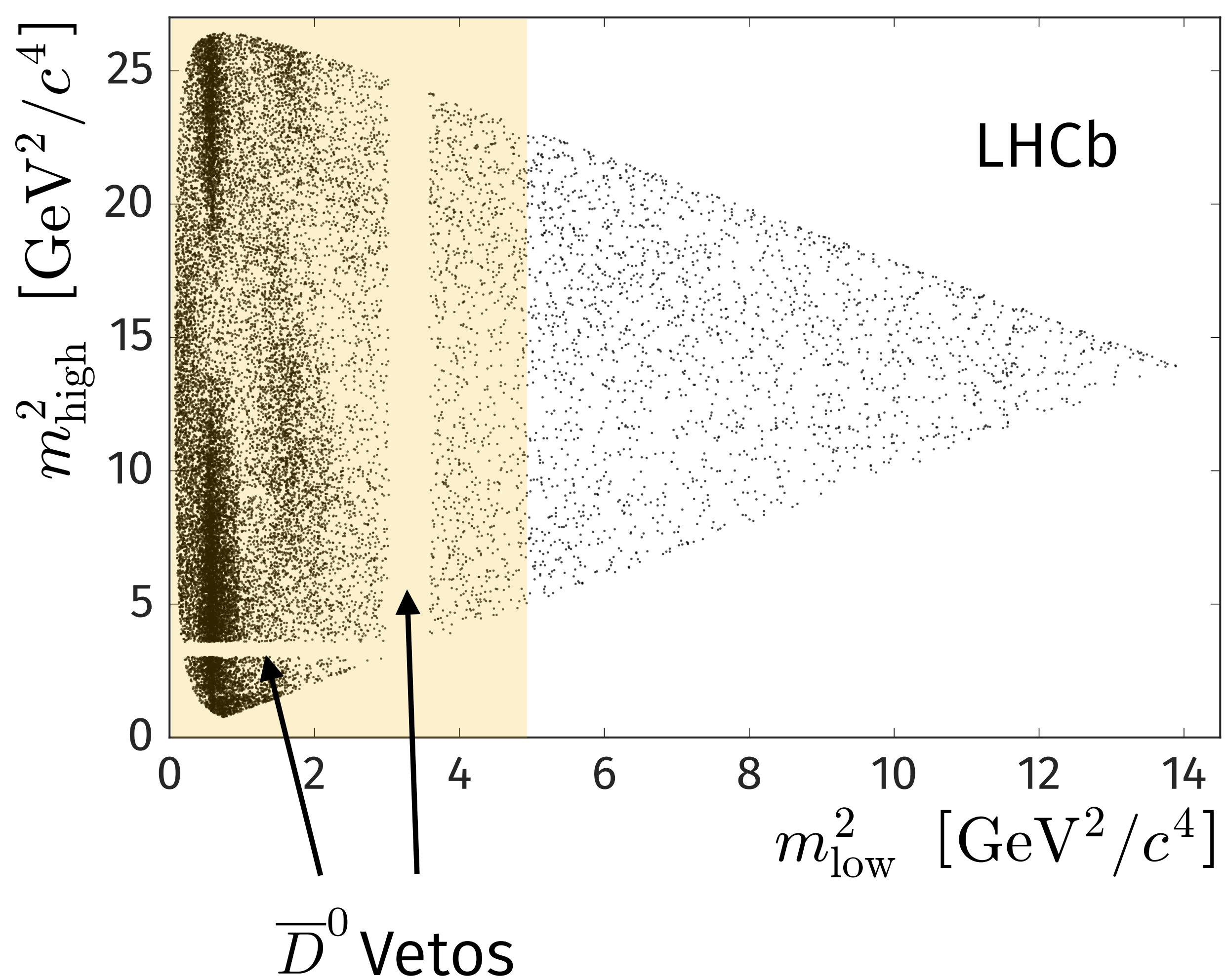

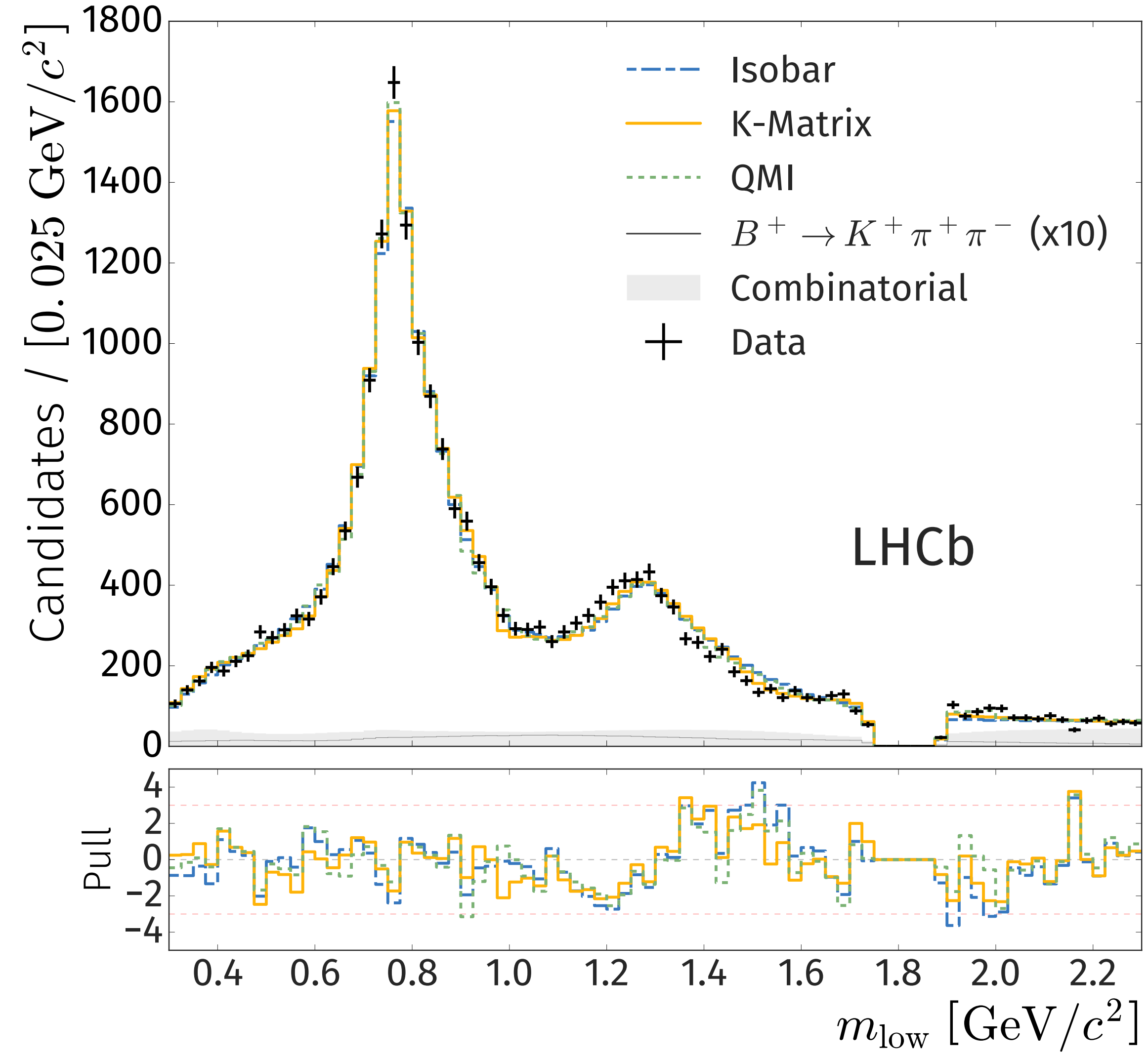

Weak decays to $\pi^+\pi^-$ and $K^+\pi^-$, narrow resonance

$B^+ \to \pi^+\pi^+\pi^-$

LHCb-PAPER-2019-017
LHCb-PAPER-2019-018

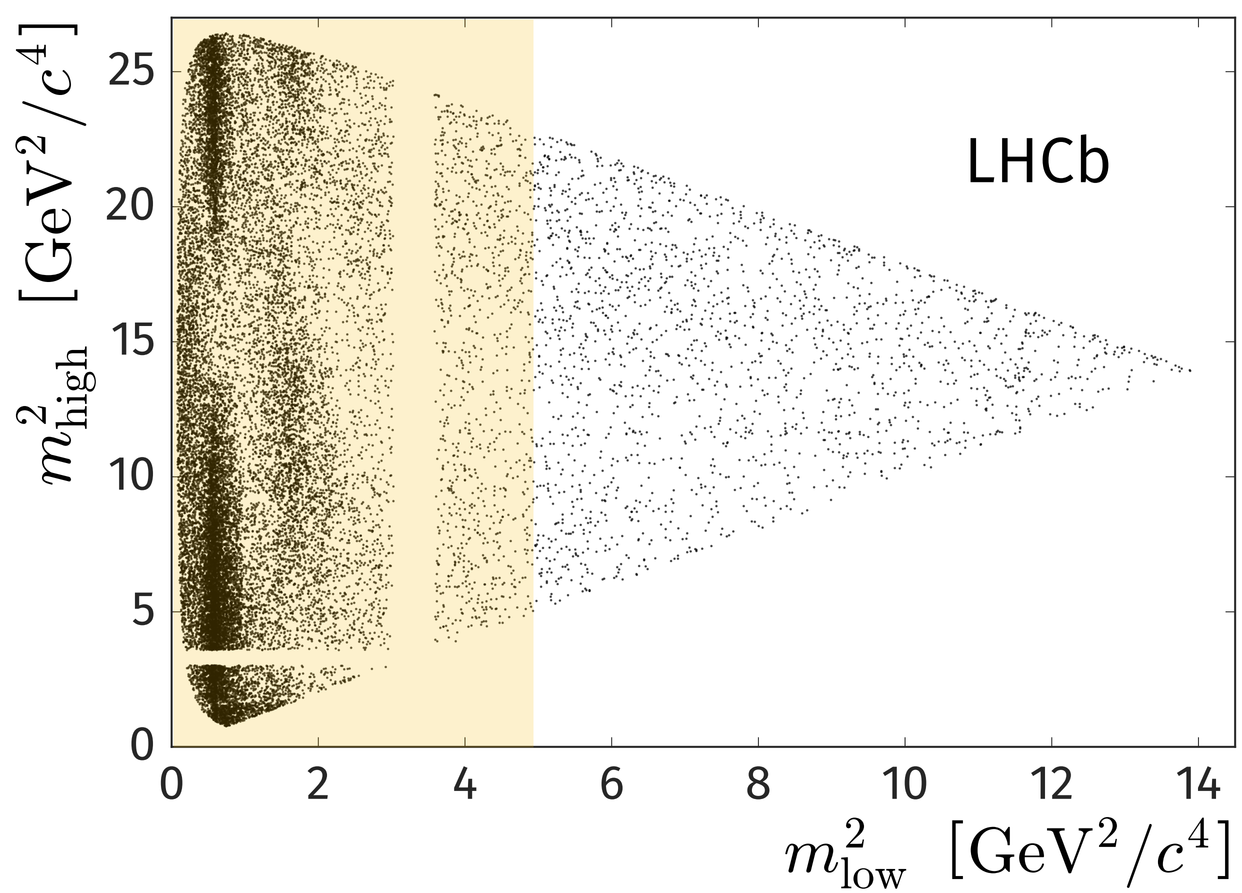

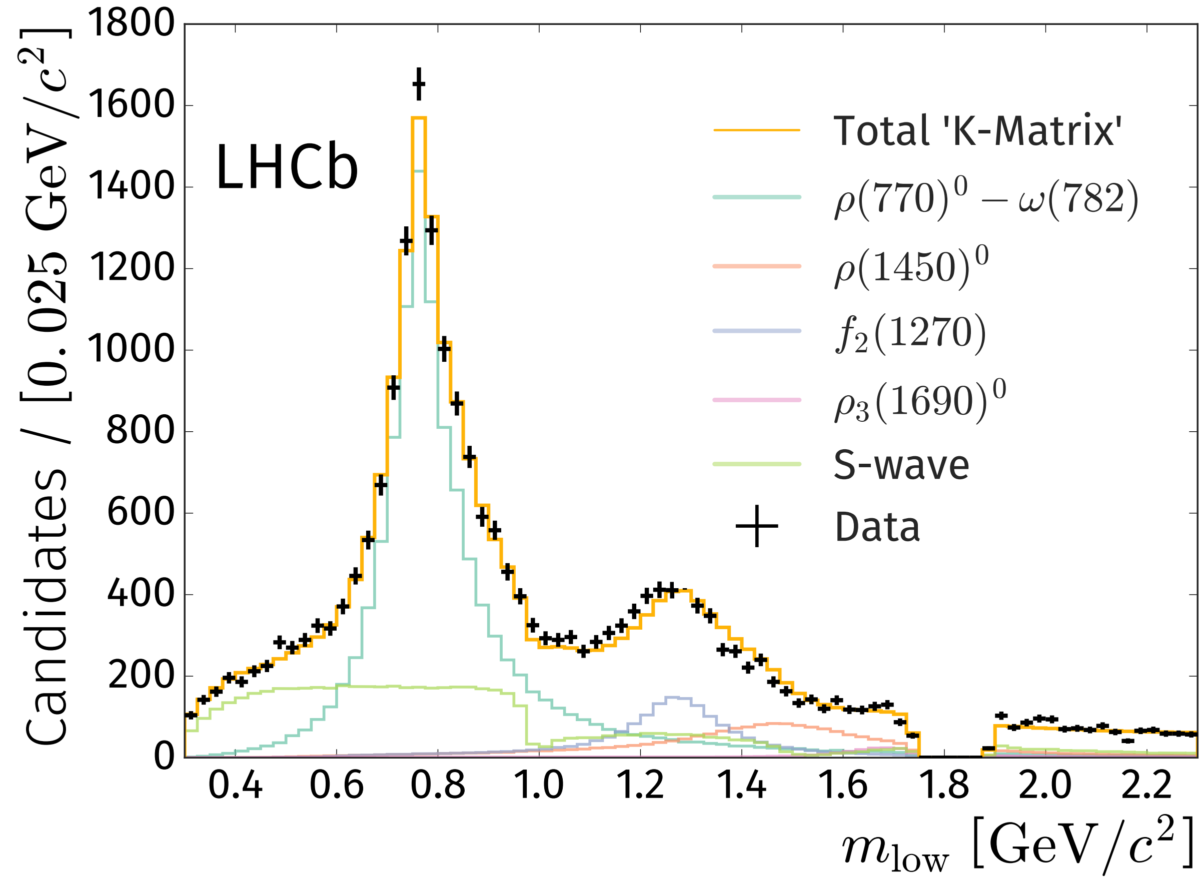

$\rho(770)^0$

- Very little asymmetry in this region as a function of **mass**:

$$\Rightarrow A_{\mathrm{CP}}(\rho(770)^0) \to 0$$

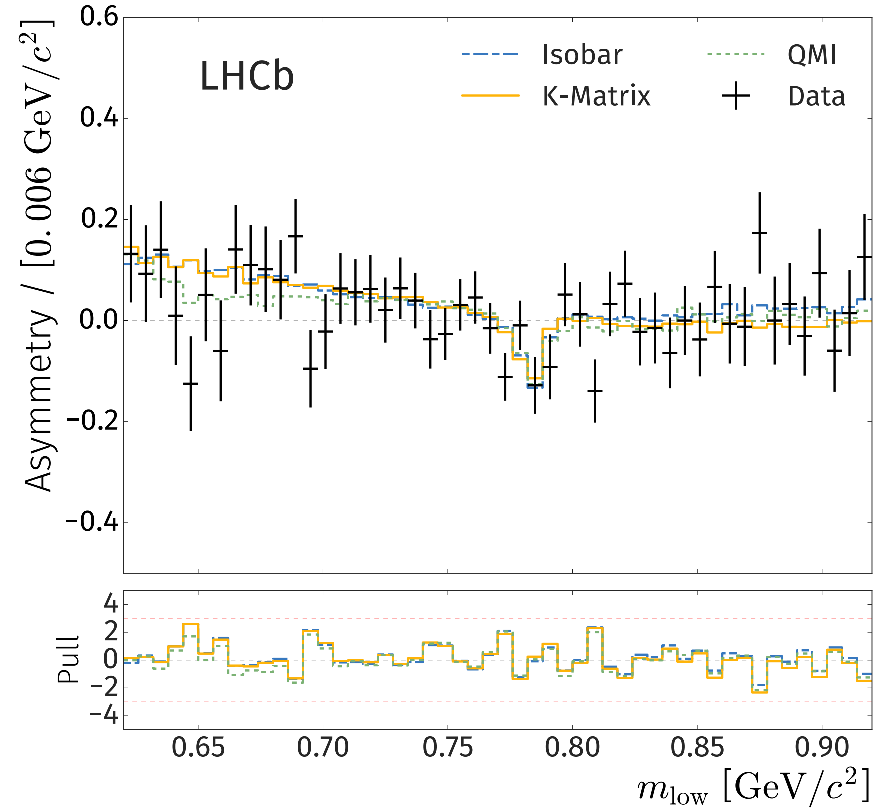

- Also very little asymmetry as a function of **helicity angle**…

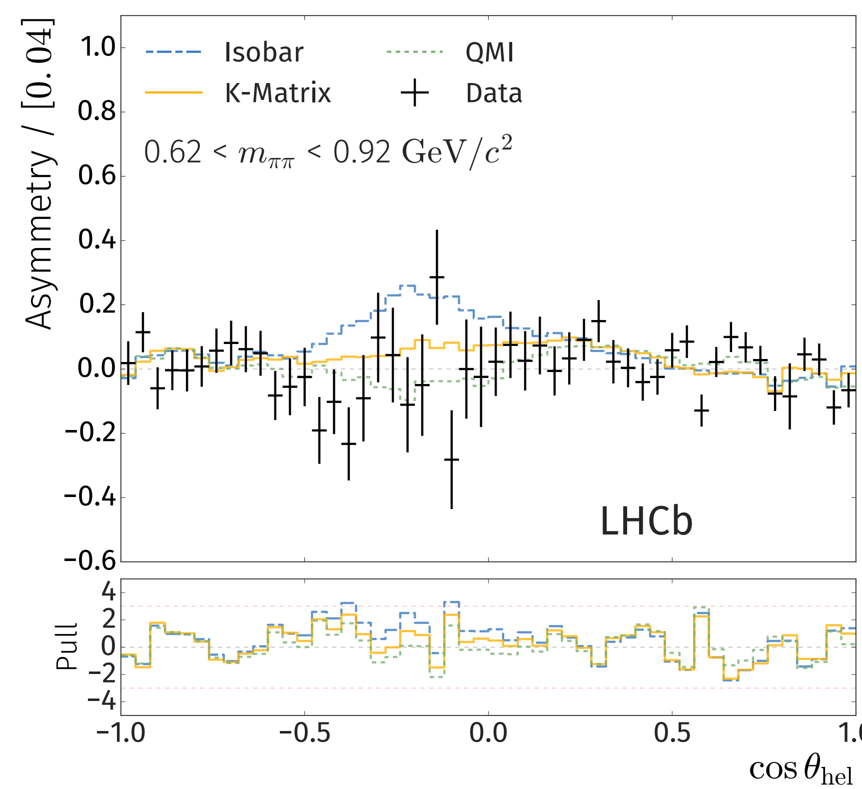

- …so **where** is the CP violation?

LHCb-PAPER-2019-017
LHCb-PAPER-2019-018

$\rho(770)^0$

LHCb-PAPER-2019-017
LHCb-PAPER-2019-018

- Below and above the $\rho(770)^0$ mass:

Below | Above

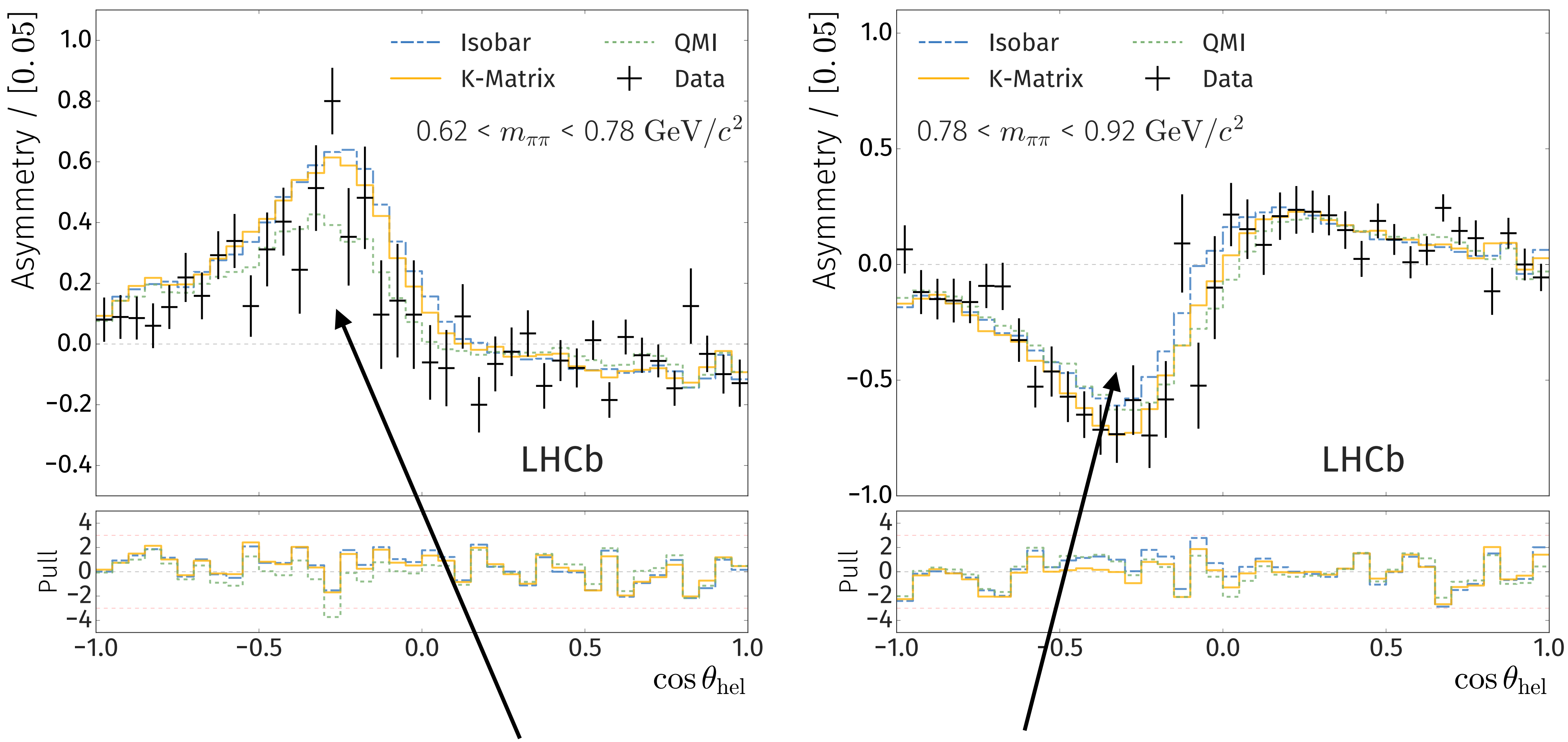

Almost perfect cancellation!

$\rho(770)^0$

LHCb-PAPER-2019-017
LHCb-PAPER-2019-018

- But why?

This region is dominated by slowly varying spin 0, and the rapidly varying spin-1 $\rho(770)^0$

Interference term between these is $\sim \cos\theta_{\text{hel}}$, when projecting on mass (integrating over $\cos\theta_{\text{hel}}$) this term **vanishes!**

CP violation is driven by the **strong phase** of the resonance, varies as a function of mass, symmetric about the pole

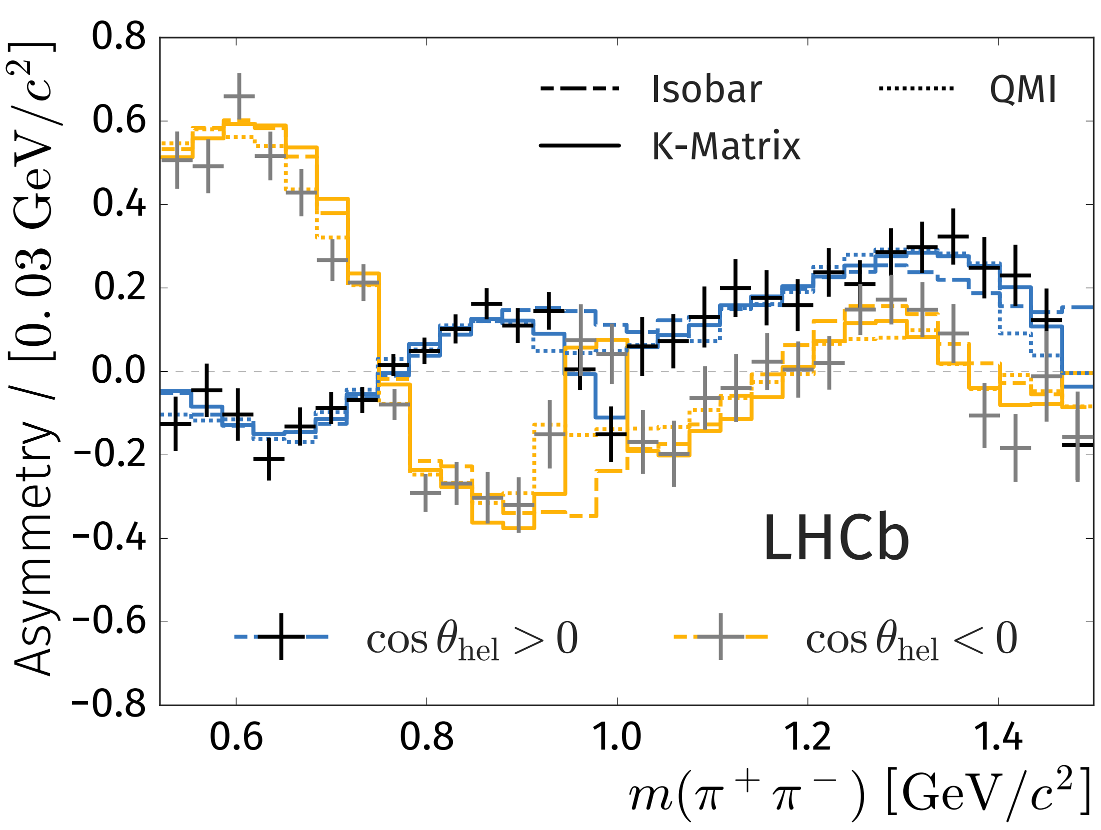

$f_2(1270)$

LHCb-PAPER-2019-017
LHCb-PAPER-2019-018

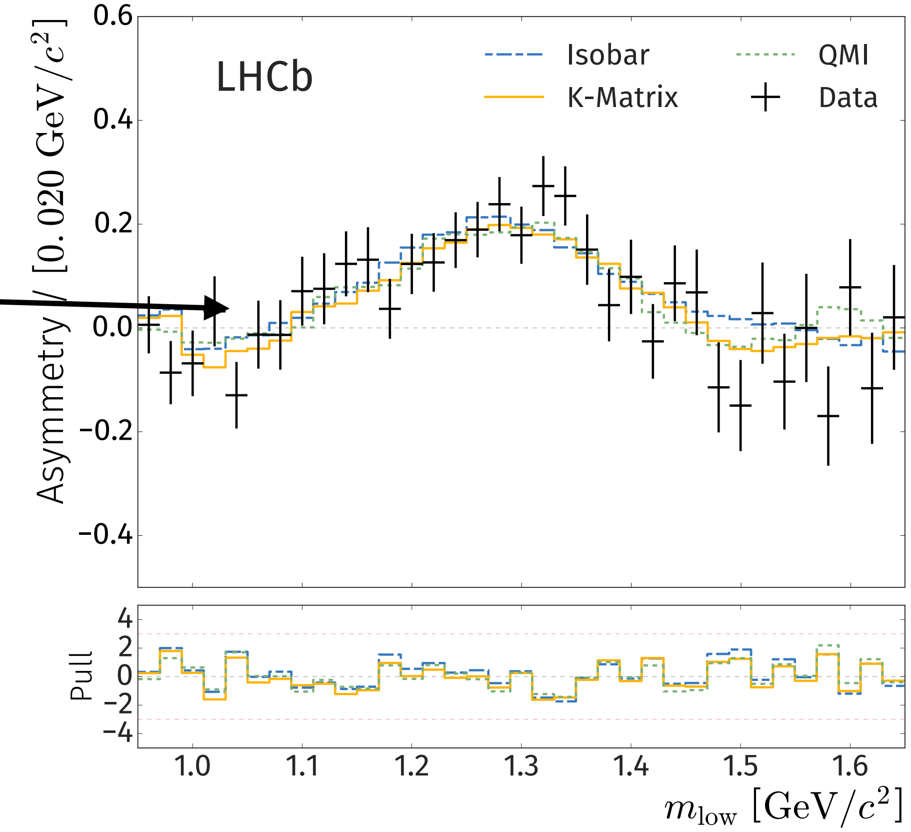

- Very large asymmetry in this region, associated with the $f_2(1270)$ component, an $A_{\rm CP}$ of around 40% in all models
- Robust to systematic effects
- One of the largest CP asymmetries ever observed!

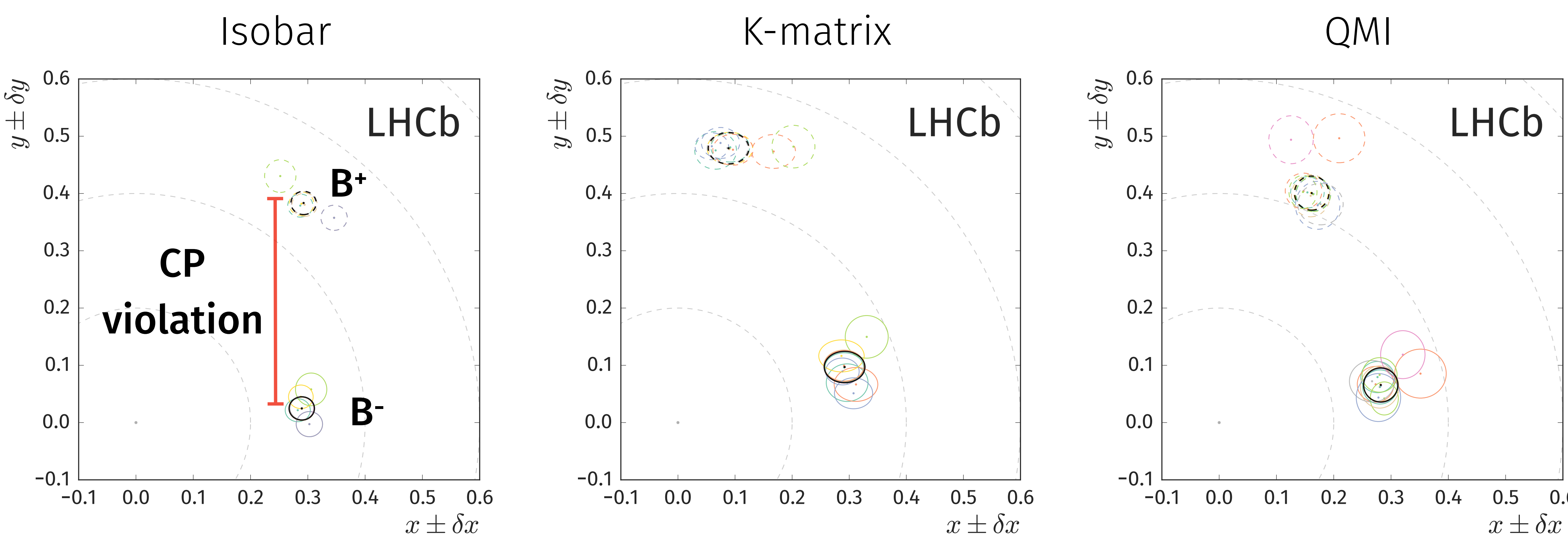

S-wave model projections - comparisons

LHCb-PAPER-2019-017
LHCb-PAPER-2019-018

No $f_0(1500)$ in the isobar model

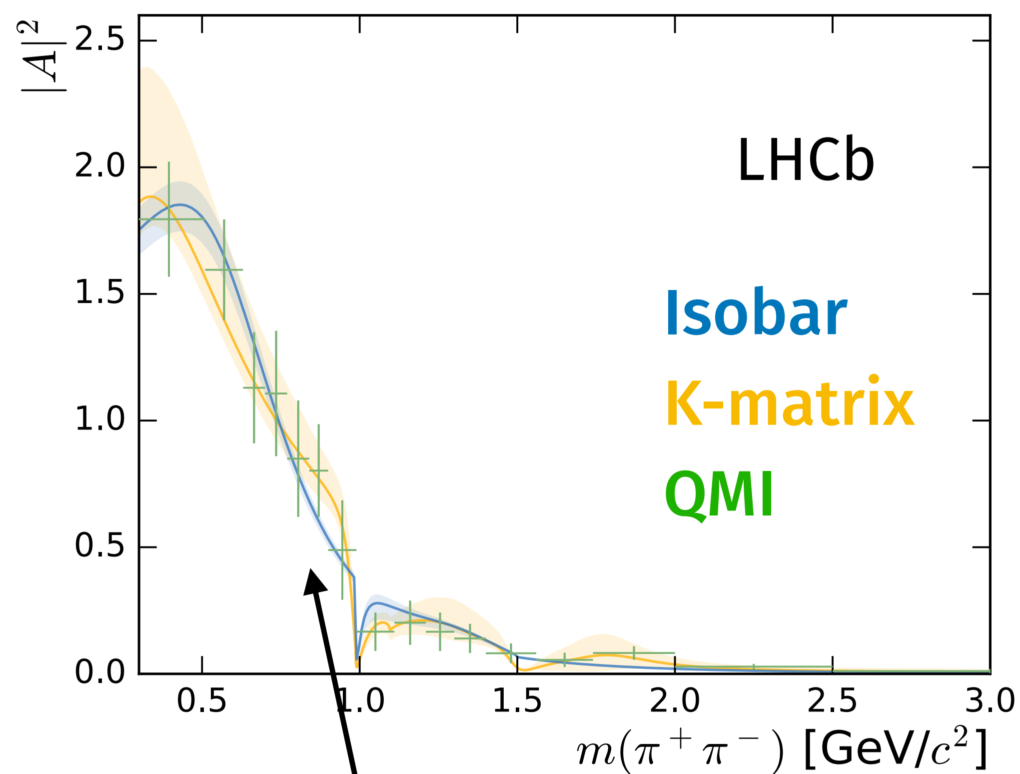

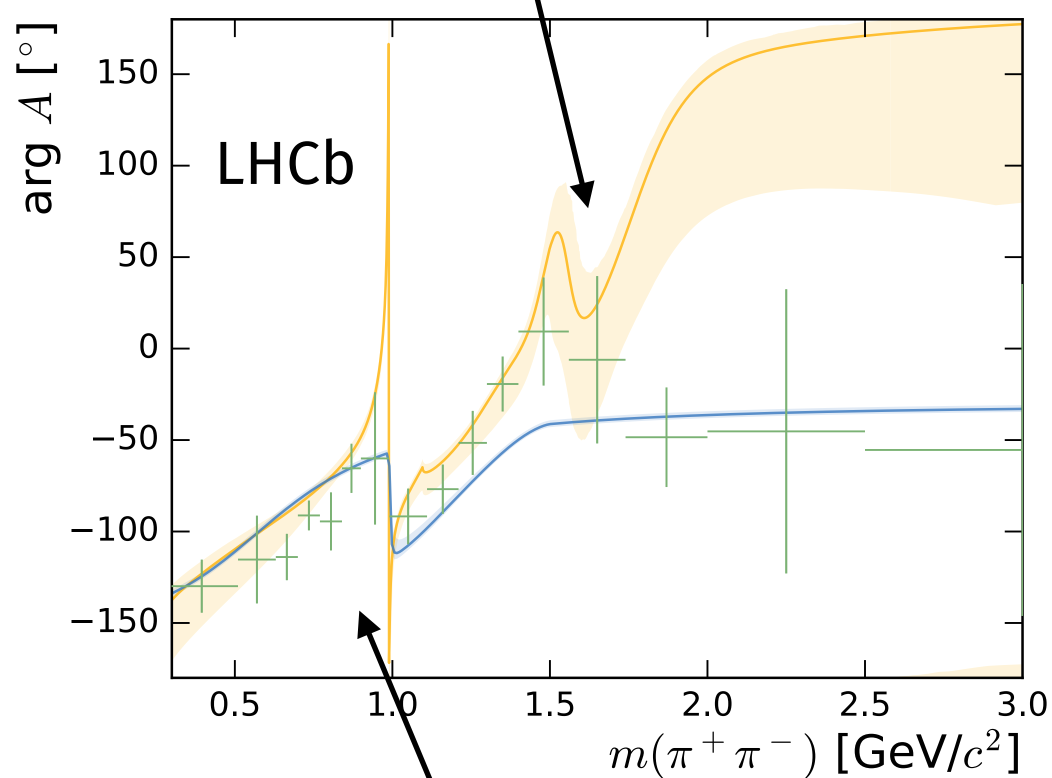

Agreement between magnitudes is very good

Phases are harder to get right, models rely on different assumptions

S-wave model projections

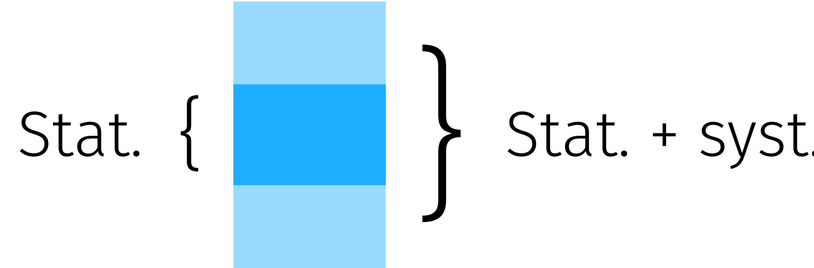

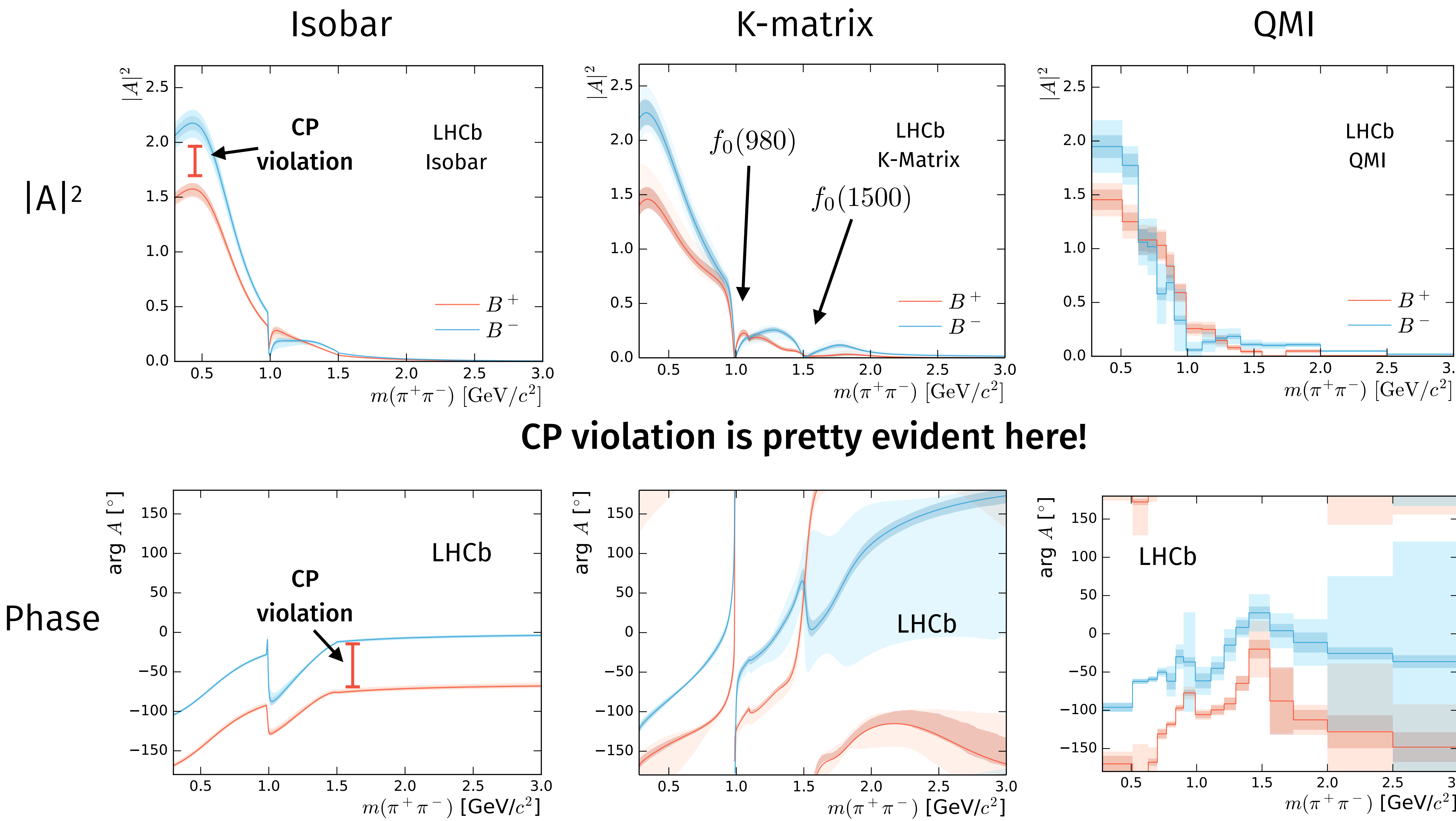

CP violation is pretty evident here!

LHCb-PAPER-2019-017
LHCb-PAPER-2019-018

Correspondence with $B^+ \to K^+\pi^+K^-$

LHCb-PAPER-2019-017
LHCb-PAPER-2019-018

- Possible for strong phase generation via **final-state re-scattering**: $\pi^+\pi^- \leftrightarrow K^+K^-$

  This would imply that there is a relation between the scalar components of the $B^+ \to K^+\pi^+K^-$ and $B^+ \to \pi^+\pi^+\pi^-$ decays

- Large CP asymmetry observed in the re-scattering (~1.0 - ~1.5 GeV) range in $B^+ \to K^+\pi^+K^-$ of around 66%, but less in $B^+ \to \pi^+\pi^+\pi^-$

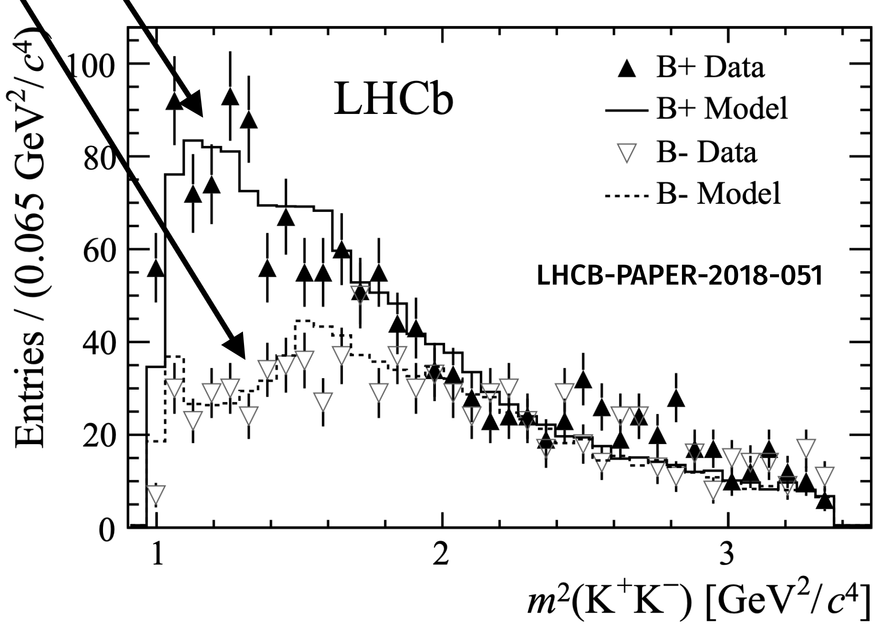

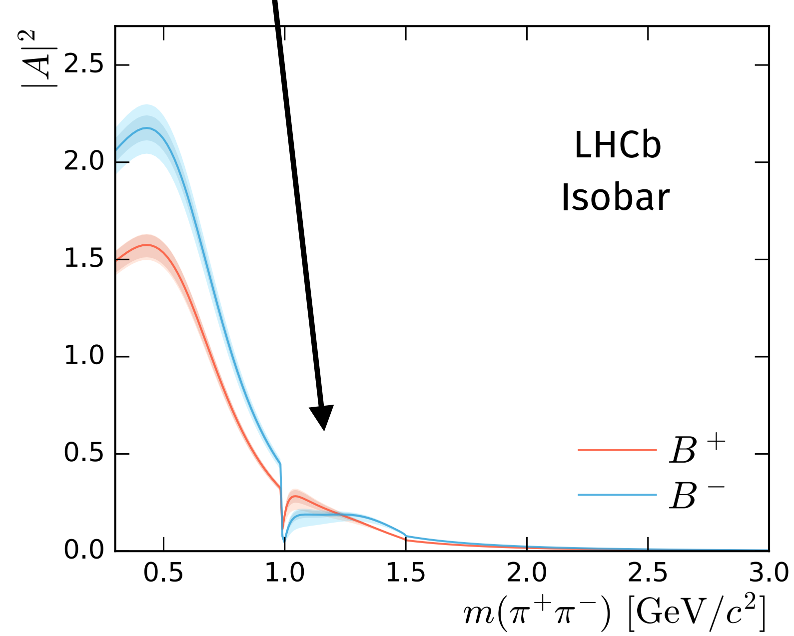

- To gain more information on this phenomenon would required a **coupled channel** analysis of both decay modes

Numerical results

LHCb-PAPER-2019-017
LHCb-PAPER-2019-018

- **Fit-fractions** - the rate if only this component contributed

Component	Isobar	K-matrix	QMI
$\rho(770)^0$	$55.5 \pm 0.6 \pm 0.7 \pm 2.5$	$56.5 \pm 0.7 \pm 1.5 \pm 3.1$	$54.8 \pm 1.0 \pm 1.9 \pm 1.0$
$\omega(782)$	$0.50 \pm 0.03 \pm 0.03 \pm 0.04$	$0.47 \pm 0.04 \pm 0.01 \pm 0.03$	$0.57 \pm 0.10 \pm 0.12 \pm 0.12$
$f_2(1270)$	$9.0 \pm 0.3 \pm 0.8 \pm 1.4$	$9.3 \pm 0.4 \pm 0.6 \pm 2.4$	$9.6 \pm 0.4 \pm 0.7 \pm 3.9$
$\rho(1450)^0$	$5.2 \pm 0.3 \pm 0.4 \pm 1.9$	$10.5 \pm 0.7 \pm 0.8 \pm 4.5$	$7.4 \pm 0.5 \pm 3.9 \pm 1.1$
$\rho_3(1690)^0$	$0.5 \pm 0.1 \pm 0.1 \pm 0.4$	$1.5 \pm 0.1 \pm 0.1 \pm 0.4$	$1.0 \pm 0.1 \pm 0.5 \pm 0.1$
S-wave	$25.4 \pm 0.5 \pm 0.7 \pm 3.6$	$25.7 \pm 0.6 \pm 2.6 \pm 1.4$	$26.8 \pm 0.7 \pm 2.0 \pm 1.0$

$$\mathcal{F}_j = \frac{\int_{\text{PhSp}} |A_j|^2 + |\overline{A}_j|^2 d\text{PhSp}}{\int_{\text{PhSp}} |\sum_j A_j|^2 + |\sum_j \overline{A}_j|^2 d\text{PhSp}}$$

- Quasi-two-body **CP asymmetries** - asymmetry of a single component

Component	Isobar	K-matrix	QMI
$\rho(770)^0$	$+0.7 \pm 1.1 \pm 1.2 \pm 1.5$	$+4.2 \pm 1.5 \pm 2.6 \pm 5.8$	$+4.4 \pm 1.7 \pm 2.3 \pm 1.6$
$\omega(782)$	$-4.8 \pm 6.5 \pm 6.6 \pm 3.5$	$-6.2 \pm 8.4 \pm 5.6 \pm 8.1$	$-7.9 \pm 16.5 \pm 14.2 \pm 7.0$
$f_2(1270)$	$+46.8 \pm 6.1 \pm 3.6 \pm 4.4$	$+42.8 \pm 4.1 \pm 2.1 \pm 8.9$	$+37.6 \pm 4.4 \pm 6.0 \pm 5.2$
$\rho(1450)^0$	$-12.9 \pm 3.3 \pm 7.0 \pm 35.7$	$+9.0 \pm 6.0 \pm 10.8 \pm 45.7$	$-15.5 \pm 7.3 \pm 14.3 \pm 32.2$
$\rho_3(1690)^0$	$-80.1 \pm 11.4 \pm 13.5 \pm 24.1$	$-35.7 \pm 10.8 \pm 8.5 \pm 35.9$	$-93.2 \pm 6.8 \pm 8.0 \pm 38.1$
S-wave	$+14.4 \pm 1.8 \pm 2.1 \pm 1.9$	$+15.8 \pm 2.6 \pm 2.1 \pm 6.9$	$+15.0 \pm 2.7 \pm 4.2 \pm 7.0$

$$A^j_{\text{CP}} = \frac{|\overline{A}_j|^2 - |A_j|^2}{|\overline{A}_j|^2 + |A_j|^2}$$

Search for CP and P violation in $\Lambda_b^0 \to p^+\pi^-\pi^+\pi^-$ decays

- CP violation has been observed in B, K, and D decays, but not yet in baryon decays
- The $\Lambda_b^0 \to p^+\pi^-\pi^+\pi^-$ decay proceeds via tree and loop diagrams with similar contributions, and via numerous intermediate resonances, enhancing the possibility for CP violation
- A previous LHCb analysis performed on Run 1 data observed a 3.3σ deviation from CP symmetry in a single triple-product asymmetry phase-space bin - this result is an update with **Run 1 + 6.6 fb^{-1} of Run 2 data**

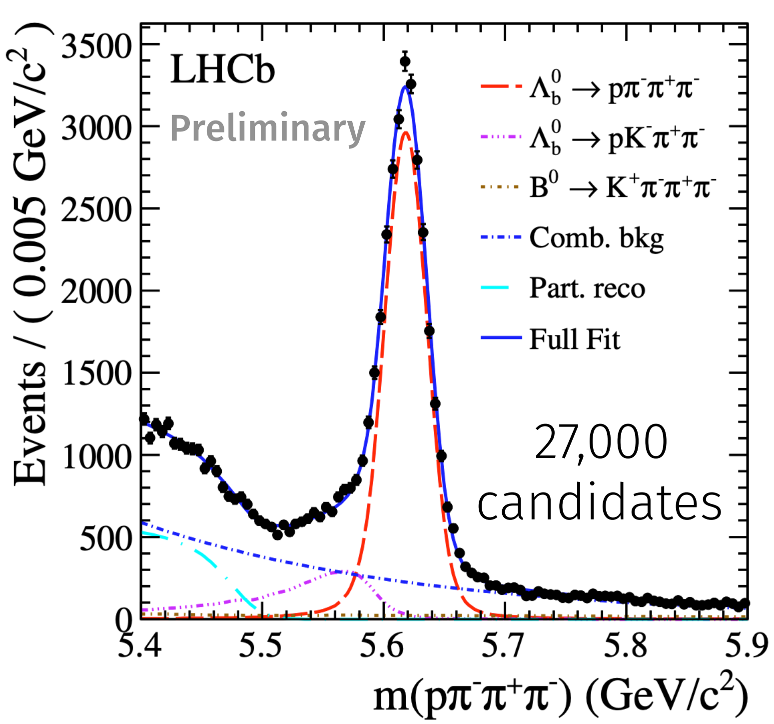

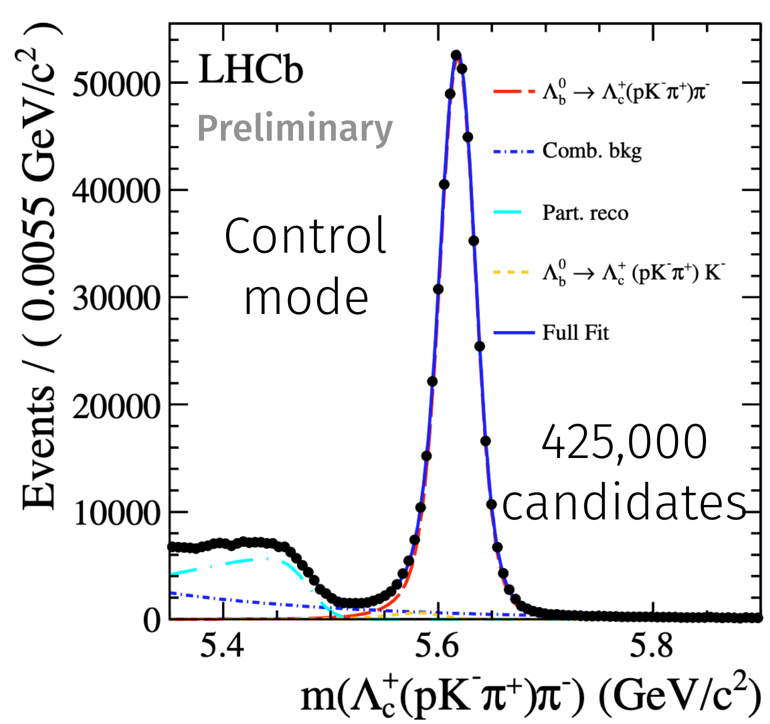

LHCb-PAPER-2019-028
(In preparation)

Search for CP and P violation in $\Lambda_b^0 \to p^+\pi^-\pi^+\pi^-$ decays

- Construct triple products of the decay product momentum

$$C_{\hat{T}} \equiv \vec{p}_{p^+} \cdot (\vec{p}_{\pi^-_{\text{fast}}} \times \vec{p}_{\pi^+})$$

and form the asymmetries according to

$$A_{\widehat{T}} = \frac{N(C_{\widehat{T}} > 0) - N(C_{\widehat{T}} < 0)}{N(C_{\widehat{T}} > 0) + N(C_{\widehat{T}} < 0)}, \qquad \overline{A}_{\widehat{T}} = \frac{\overline{N}(-\overline{C}_{\widehat{T}} > 0) - \overline{N}(-\overline{C}_{\widehat{T}} < 0)}{\overline{N}(-\overline{C}_{\widehat{T}} > 0) + \overline{N}(-\overline{C}_{\widehat{T}} < 0)},$$

with the P and CP violating observables

$$a_P^{\widehat{T}\text{-odd}} = \frac{1}{2}\left(A_{\widehat{T}} + \overline{A}_{\widehat{T}}\right), \; a_{CP}^{\widehat{T}\text{-odd}} = \frac{1}{2}\left(A_{\widehat{T}} - \overline{A}_{\widehat{T}}\right).$$

- Computed in bins of $|\Phi|$, the angle between $p^+\pi^-_{\text{fast}}$ and $\pi^+\pi^-_{\text{slow}}$ (A) and as a function of the polar and azimuthal angles (B) of the proton or Δ^{++} in the Δ^{++} or N^{*+} rest frame, in regions dominated by the (1) a_1 resonance or (2) N^{*+} resonance

LHCb-PAPER-2019-028
(In preparation)

Search for CP and P violation in $\Lambda_b^0 \to p^+\pi^-\pi^+\pi^-$ decays

- No evidence for CP violation in any region of the phase space, for any binning scheme

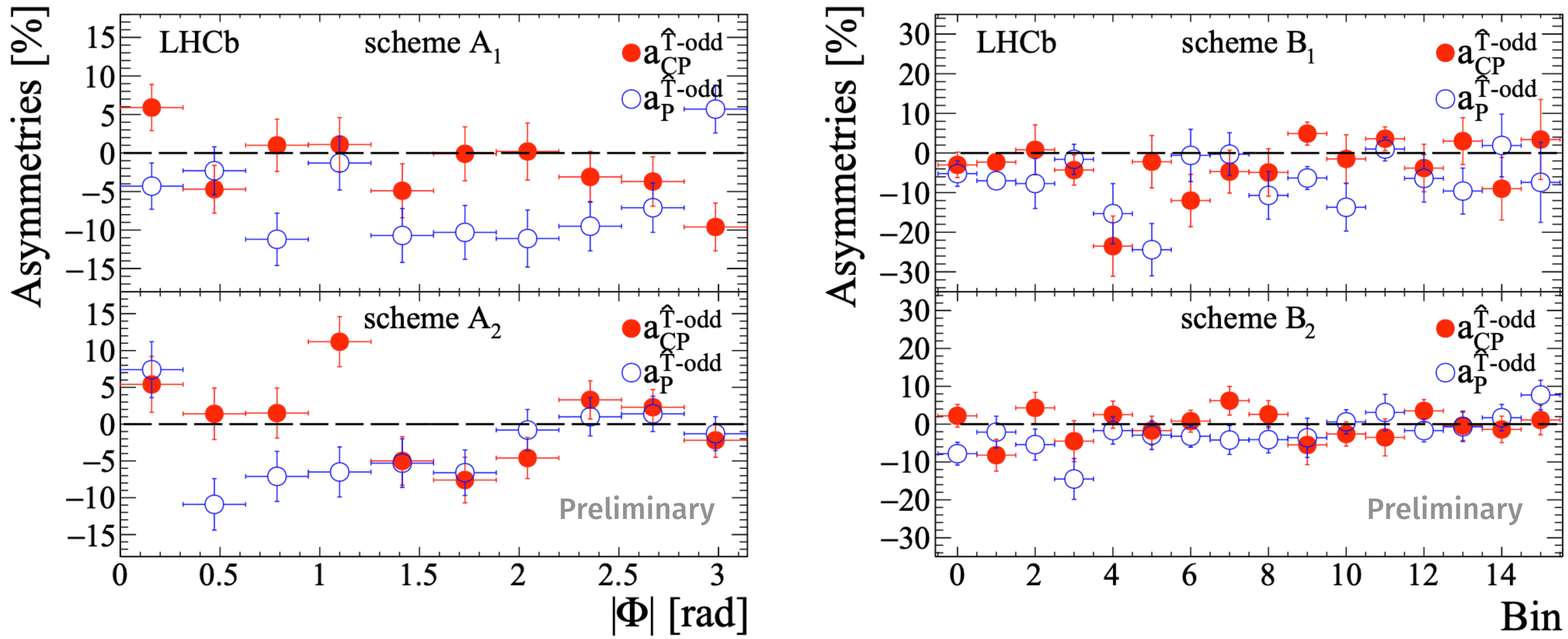

- However, for the region dominated by the $\Lambda_b^0 \to p^+ a_1(1260)^-$ decay, **P violation** on the level of **5.5σ** is observed - the **first observation** of P violation in a b-baryon decay

Asymmetry [%]	Measurement
$A_{\hat{T}}$	$-4.68 \pm 0.99 \pm 0.24$
$\bar{A}_{\hat{T}}$	$-3.29 \pm 0.99 \pm 0.24$
$a_P^{\hat{T}\text{-odd}}$	$-3.98 \pm 0.70 \pm 0.17$
$a_{CP}^{\hat{T}\text{-odd}}$	$-0.70 \pm 0.70 \pm 0.17$

Preliminary

LHCb-PAPER-2019-028
(In preparation)

Search for CP and P violation in $\Lambda_b^0 \to p^+\pi^-\pi^+\pi^-$ decays

- An additional test is performed on the same dataset, using the 'energy' test statistic

$$T \equiv \frac{1}{2n(n-1)}\sum_{i\neq j}^{n}\psi_{ij} + \frac{1}{2\overline{n}(\overline{n}-1)}\sum_{i\neq j}^{\overline{n}}\psi_{ij} - \frac{1}{n\overline{n}}\sum_{i=1}^{n}\sum_{j=1}^{\overline{n}}\psi_{ij},$$

where $\psi_{ij} = \exp(-d_{ij}^2/\delta^2)$, d_{ij} is the distance between candidates i and j, and the value of δ is the characteristic length scale of the kernel (1.6, 2.7, or 13 GeV^2/c^4)

- p-value is constructed using a permutation test, with data split using the sign of $C_{\hat{T}}$ (for P-odd test), or Λ_b^0 flavour (P-even test)

Table 3: p-values for the energy test.

Preliminary

δ	1.6 GeV^2/c^4	2.7 GeV^2/c^4	13 GeV^2/c^4
p-value (CP-conservation, P-even)	0.031	0.0027	0.013
p-value (CP-conservation, P-odd)	0.15	0.069	0.065
p-value (P-conservation)	1.3×10^{-7}	4.0×10^{-7}	0.16

> 5σ significance

LHCb-PAPER-2019-028
(In preparation)

Summary

- Multi-body decays are the place to study CP violation

  Access to overlapping resonances **enhances CP violation**, but also permits measurements of the relative phases

- Observations of large CP violation, and the **first observation** of CP violation in the interference between resonances in the $B^+ \to \pi^+\pi^+\pi^-$ decay

  Provides information on how CP violation manifests in practice - useful for understanding the (essential) **QCD components**, and informs **future studies** (e.g., in charm and baryon decays)

- **First observation** of parity violation in the decay of a b-baryon in the analysis of $\Lambda_b^0 \to p^+\pi^-\pi^+\pi^-$ decays, at the level of 5σ, although no evidence for CP violation

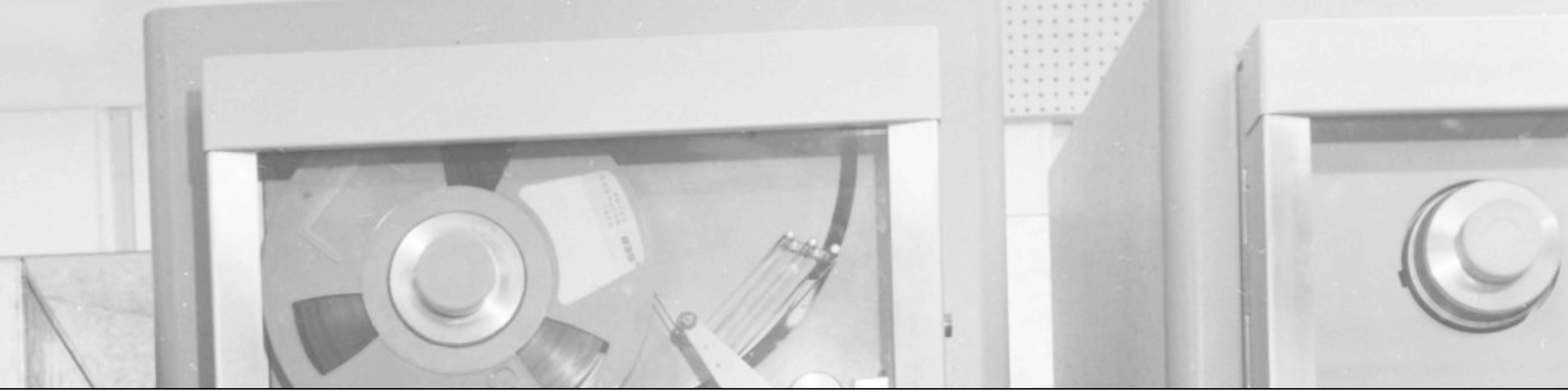

Backup

CERN PhotoLab

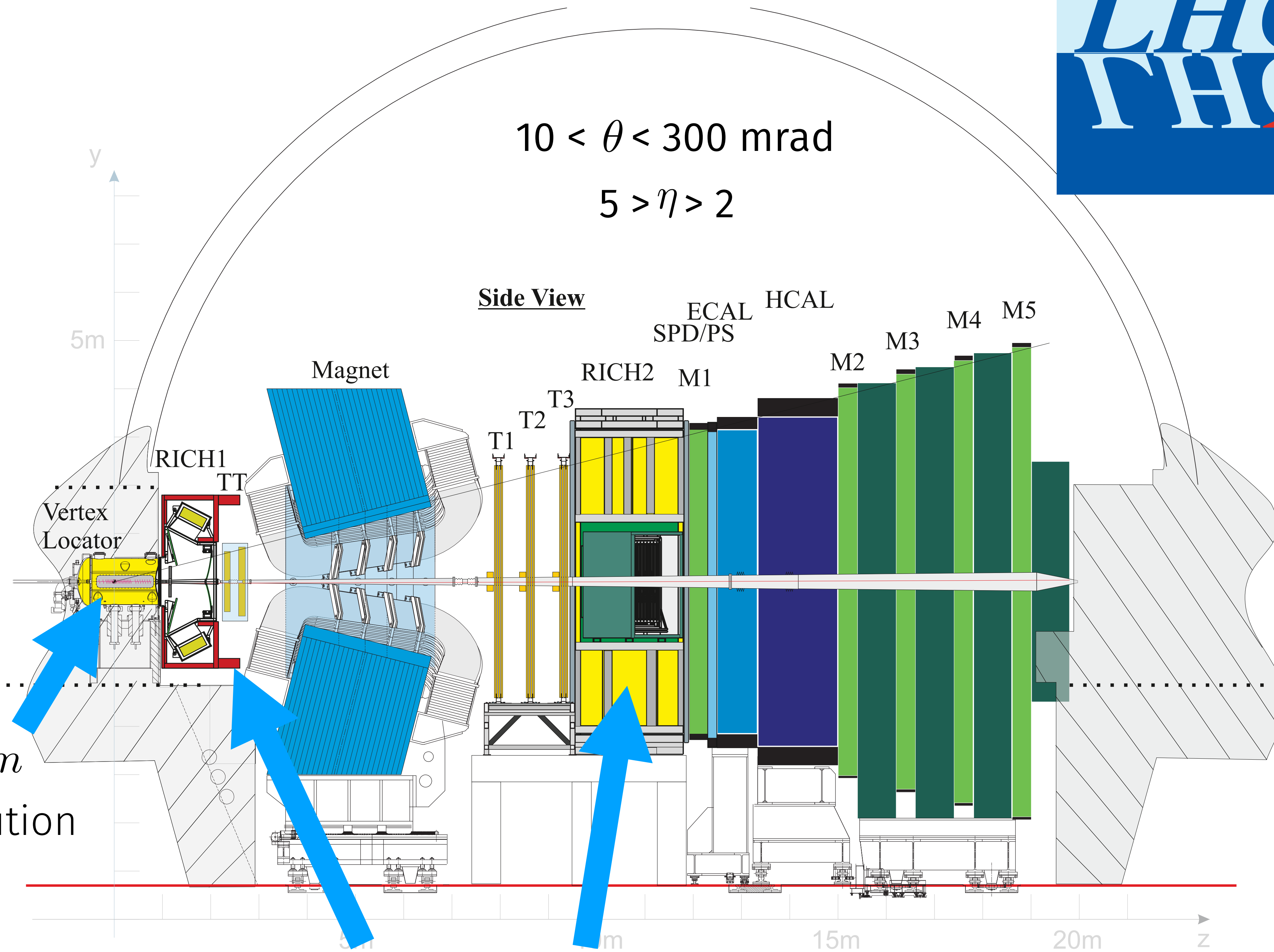

$\sim 20\ \mu m$

IP resolution

Separation of charged hadron species via Cherenkov radiation

Relativistic Breit-Wigner

$$R(m) = \frac{1}{(m_0^2 - m^2) - i m_0 \Gamma_0}$$

For:

$$m_0 = 770\,\mathrm{MeV}$$

$$\Gamma_0 = 20\,\mathrm{MeV}$$

$\lvert R(m) \rvert^2$	$\arg\left[R(m)\right]$	$\mathrm{Re}[R(m)]\,,\ \mathrm{Im}[R(m)]$
Intensity	Phase	Argand diagram

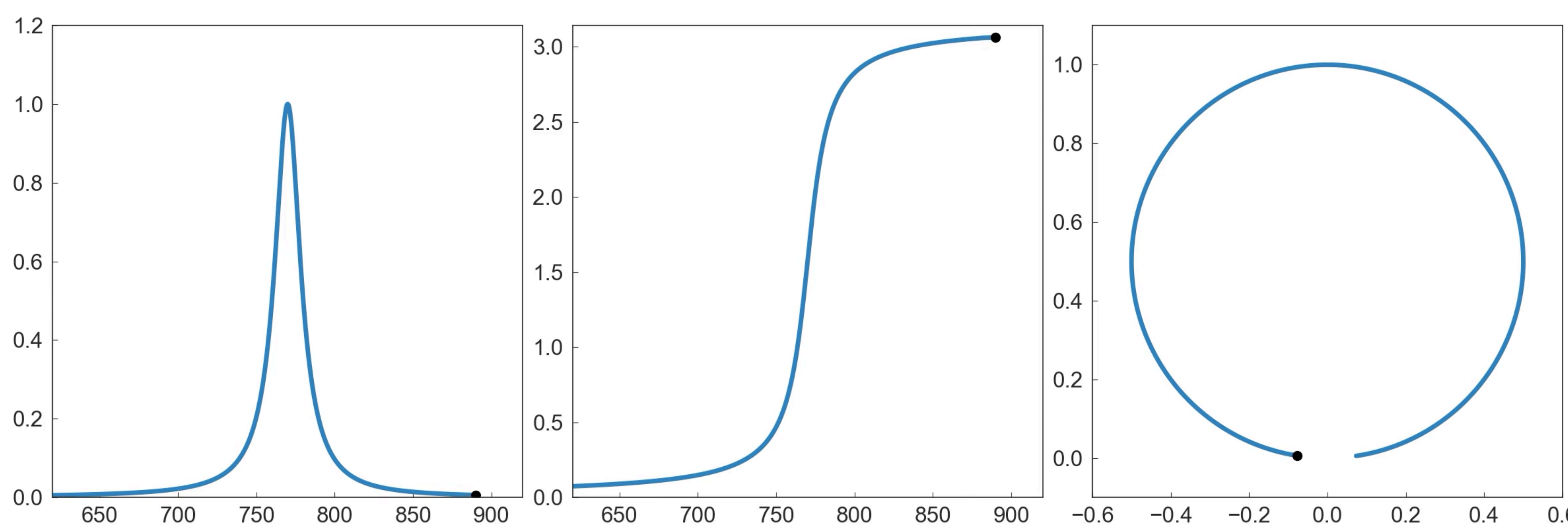

Problems with this

- Resonances near **open decay channels** see a drop in amplitude due to conservation of **unitarity** - total probability to decay to **all** channels must be conserved

- Unitarity is also violated for nearby **overlapping resonances** of the same spin

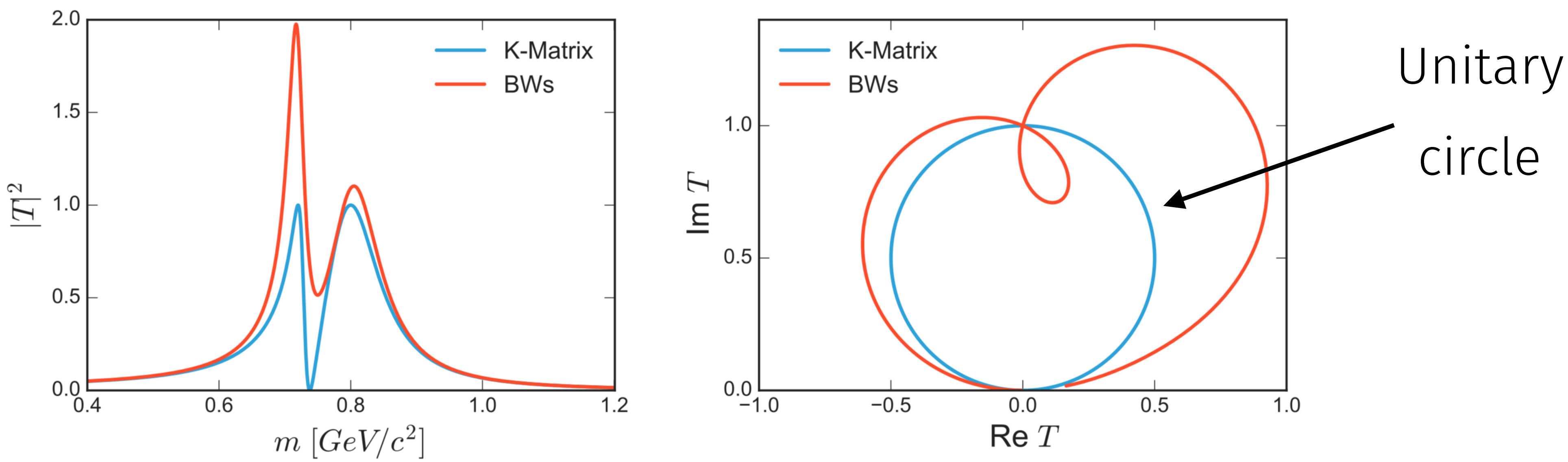

- 'Pole' masses and widths of resonances **near thresholds** are also not well replicated by Breit-Wigner lineshapes

$\rho(770)^0$

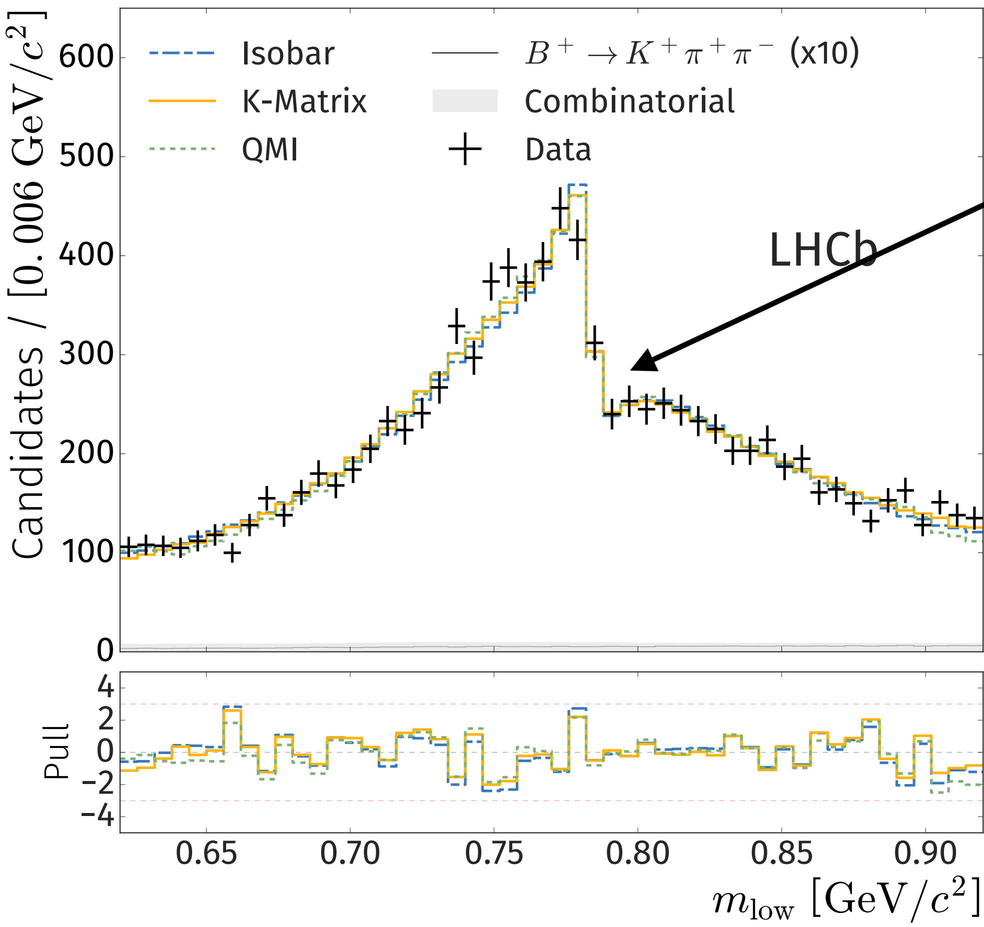

$\rho(770)^0 - \omega(782)$
Mixing

$\omega(782)$ is forbidden to decay to $\pi^+\pi^-$ due to isospin conservation

However, it can **mix** with the $\rho(770)^0$, causing a drop in the $\rho(770)^0$ amplitude above the mass of the $\omega(782)$

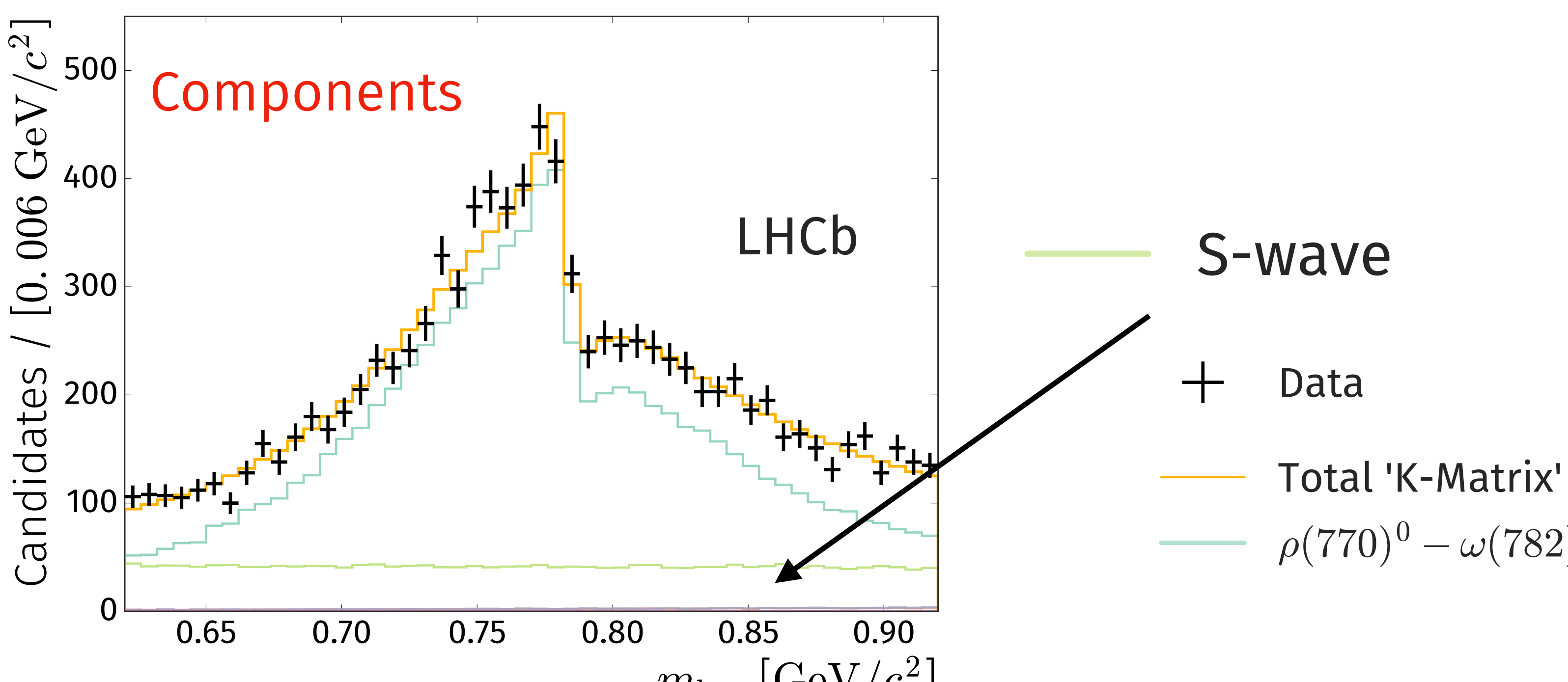

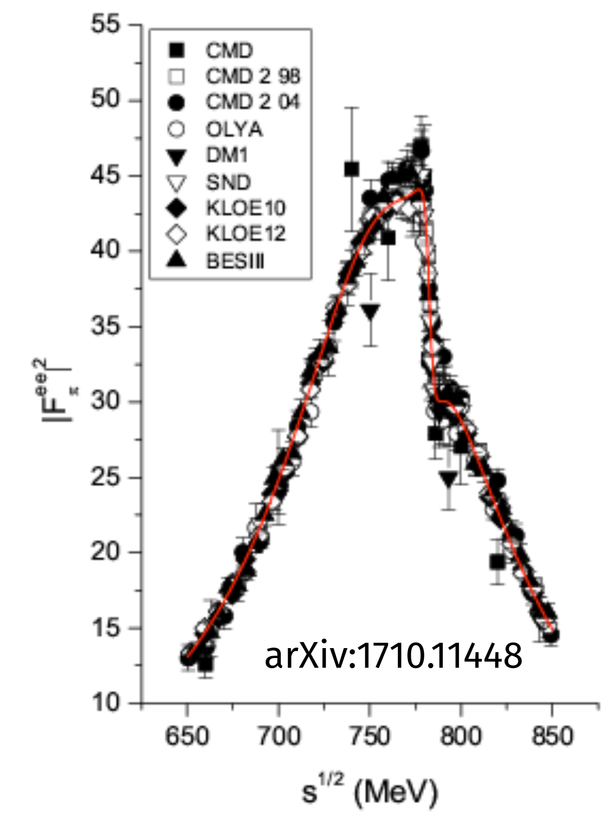

$B^+ \to \pi^+\pi^+\pi^-$

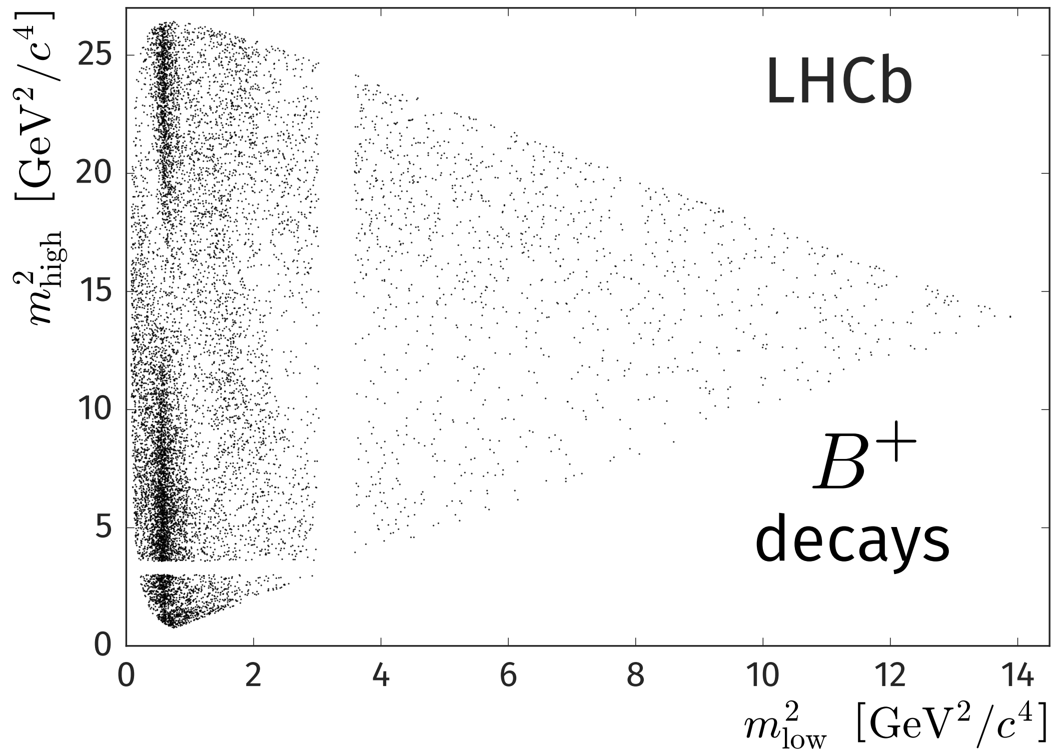

LHCb
B^+
decays
m^2_{high} [GeV$^2/c^4$]
m^2_{low} [GeV$^2/c^4$]

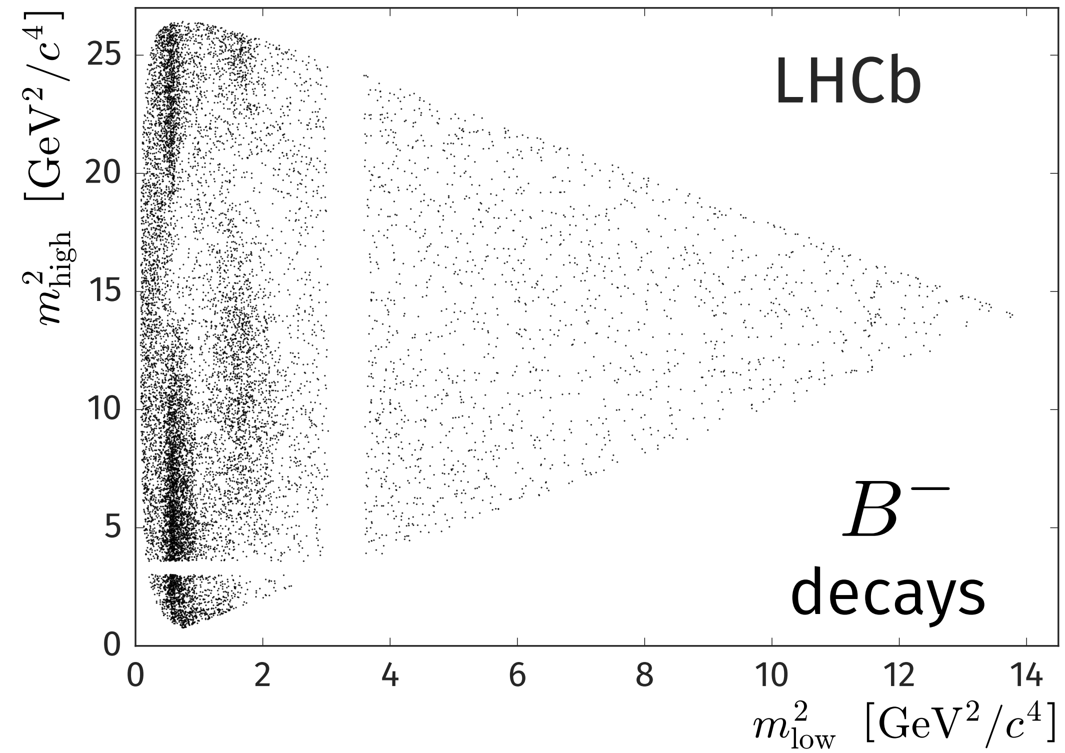

LHCb
B^-
decays
m^2_{high} [GeV$^2/c^4$]
m^2_{low} [GeV$^2/c^4$]

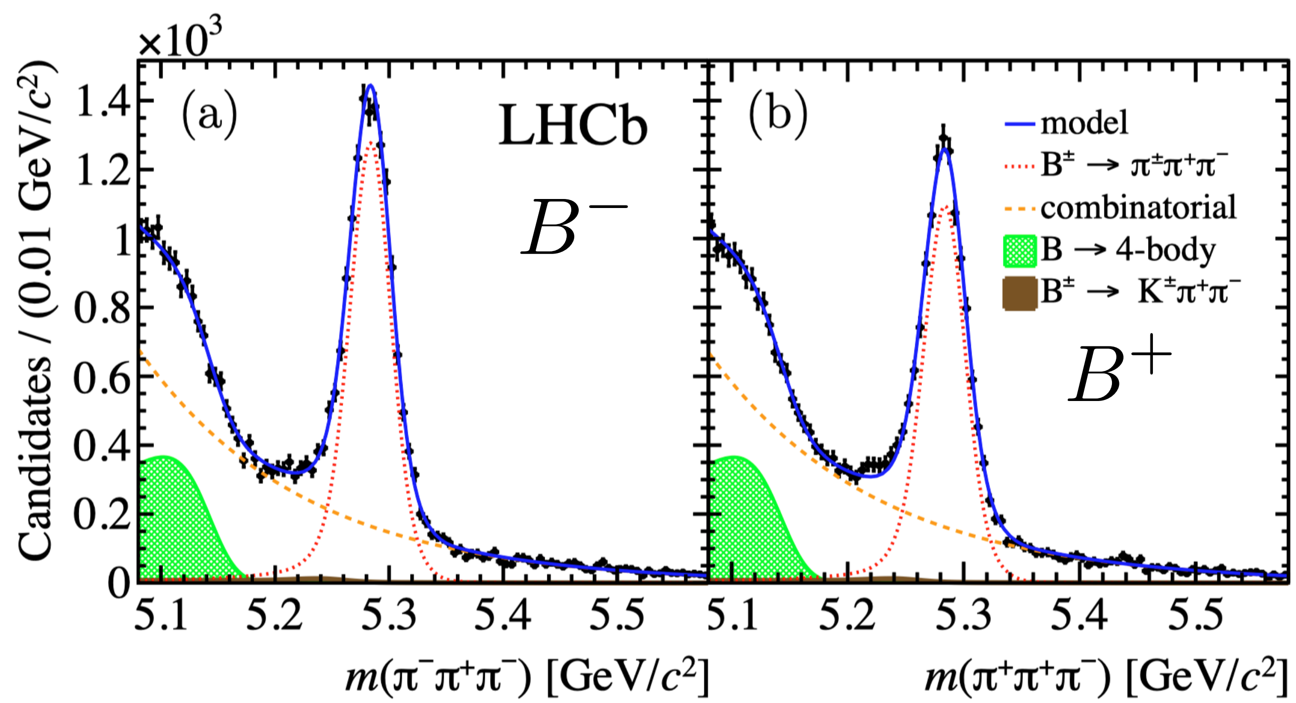

×10^3
(a)
LHCb
B^-
(b)
model
$B^\pm \to \pi^\pm\pi^+\pi^-$
combinatorial
$B \to$ 4-body
$B^\pm \to K^\pm\pi^+\pi^-$
B^+
Candidates / (0.01 GeV/c^2)
$m(\pi^-\pi^+\pi^-)$ [GeV/c^2]
$m(\pi^+\pi^+\pi^-)$ [GeV/c^2]

f2 width

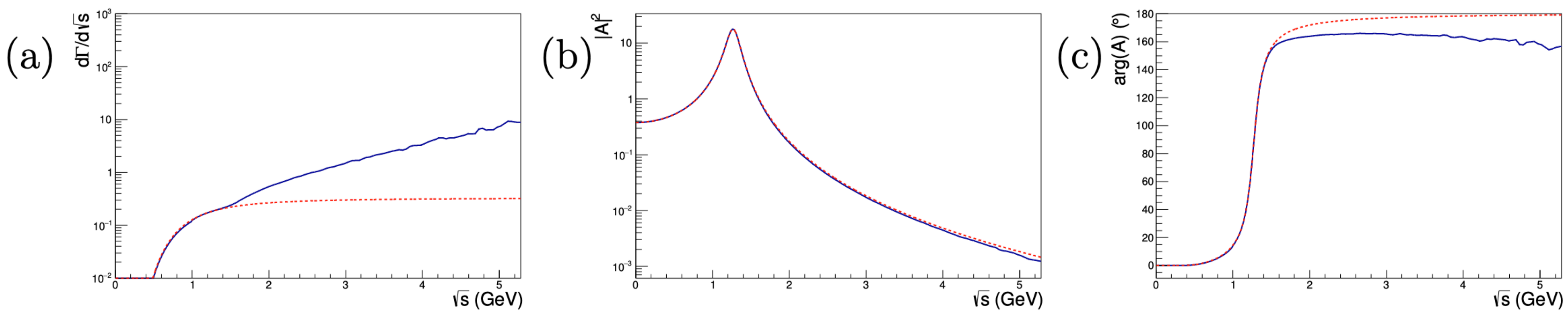

Figure 99: Comparison of the mass-dependence of the (a) $f_2(1270)$ total width (blue) with its $\pi^+\pi^-$ partial width (red), and its effects on (b), the Breit-Wigner amplitude-squared and (c) the Breit-Wigner phase

f2 width

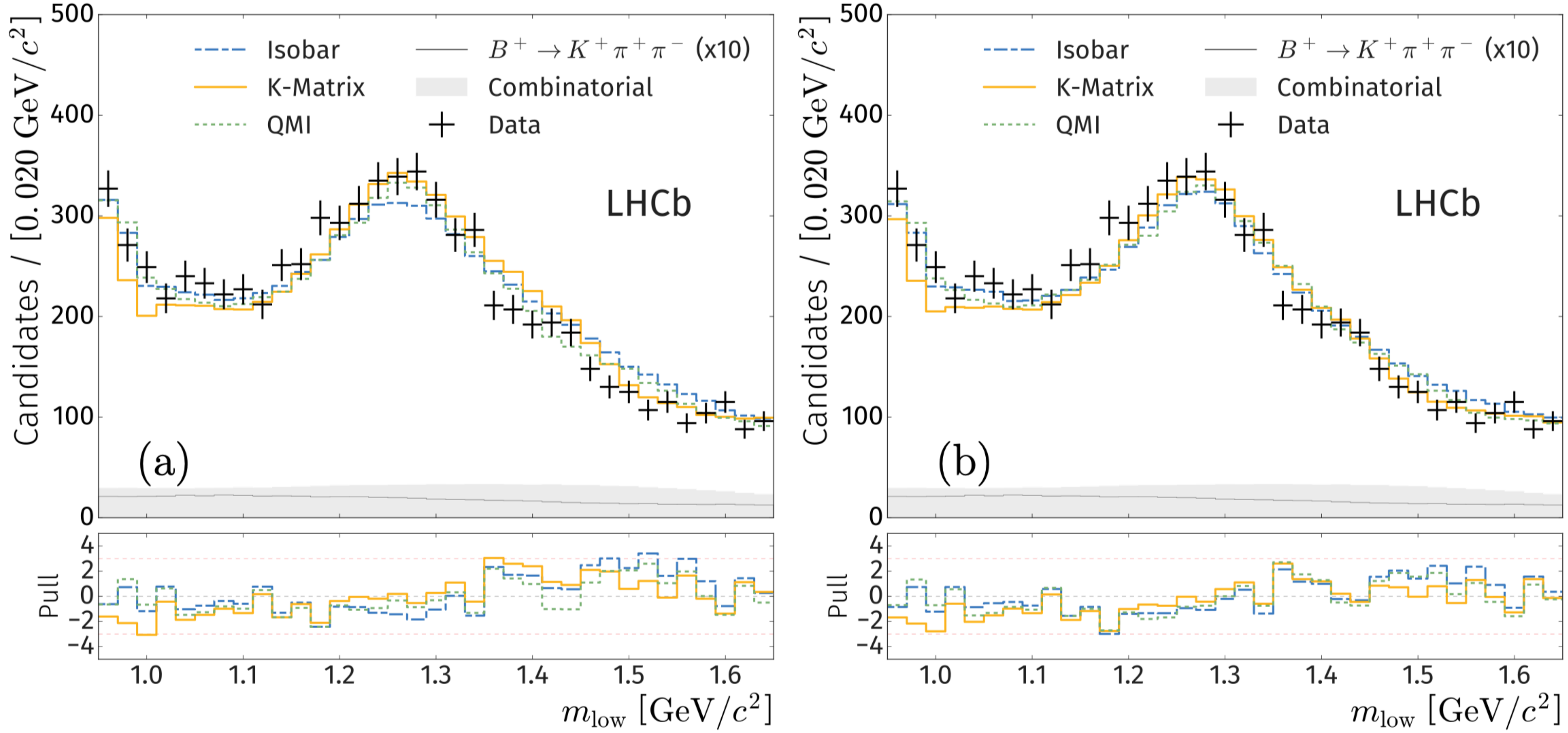

Figure 15: Data and fit model projections in the $f_2(1270)$ region with (a) freely varied $f_2(1270)$ resonance parameters, and (b) with an additional spin-2 component with mass and width parameters determined by the fit.

Backgrounds and efficiencies

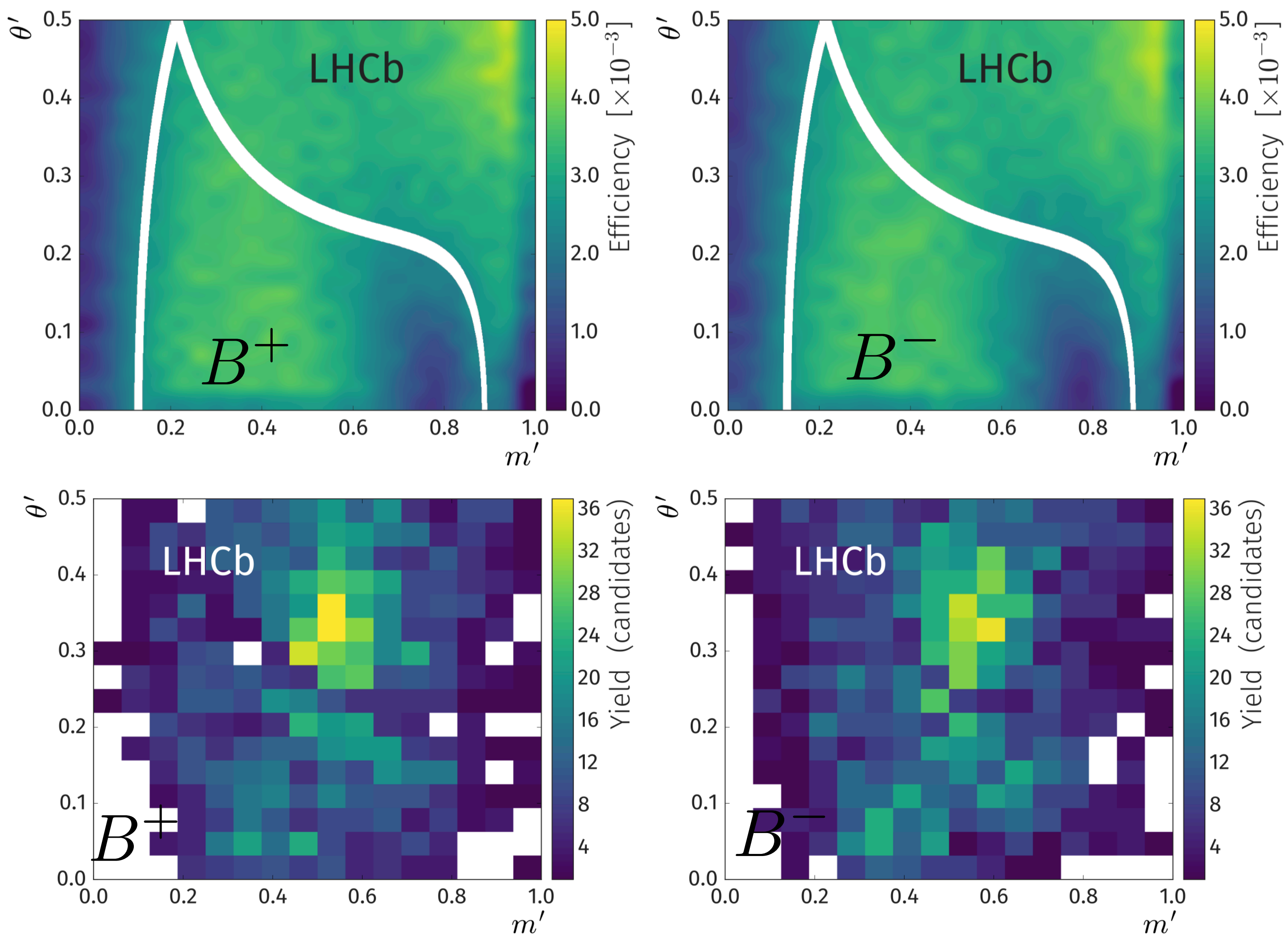

$B^+ \to K^+\pi^+\pi^-$

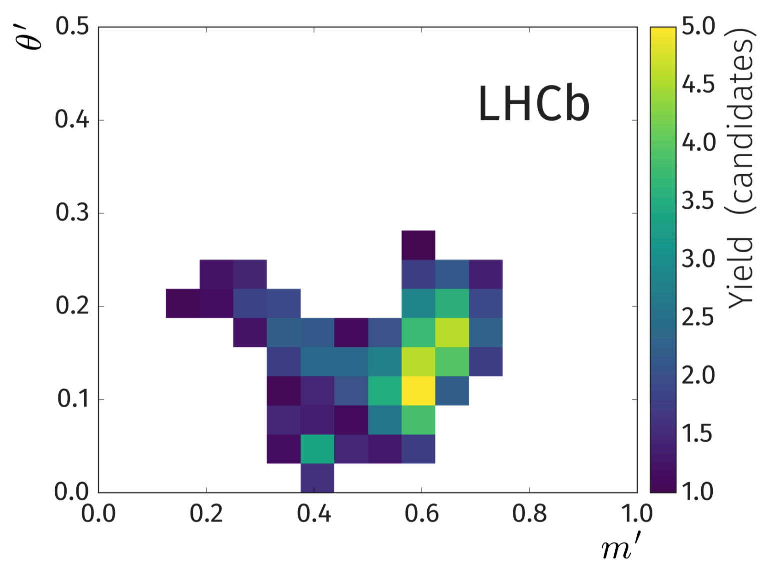

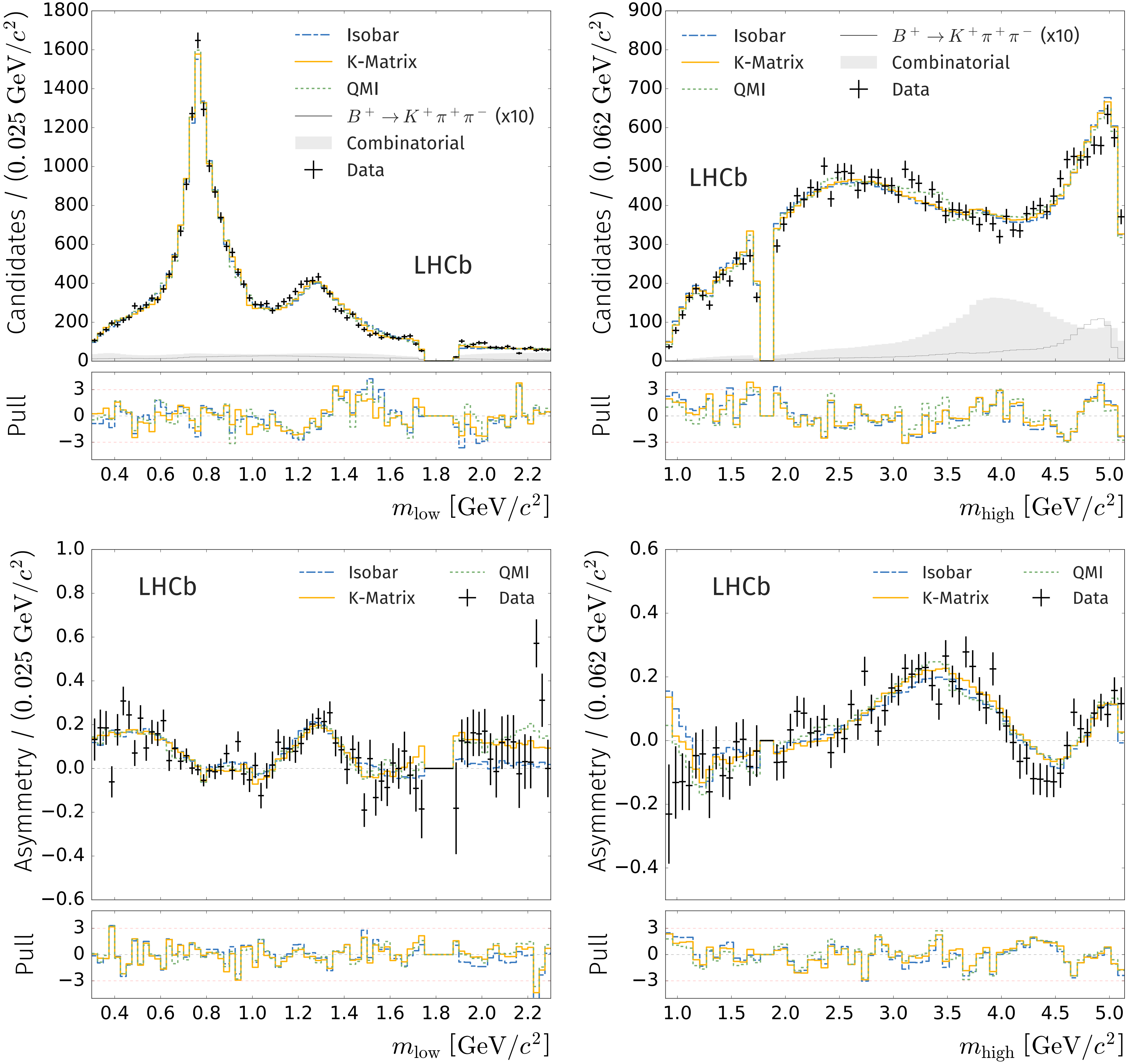

Candidates / (0.025 GeV/c^2)
Isobar
K-Matrix
QMI
$B^+ \to K^+\pi^+\pi^-$ (x10)
Combinatorial
Data
LHCb
Pull
$m_{\rm low}$ [GeV/c^2]
Candidates / (0.062 GeV/c^2)
$m_{\rm high}$ [GeV/c^2]
Asymmetry / (0.025 GeV/c^2)
Asymmetry / (0.062 GeV/c^2)

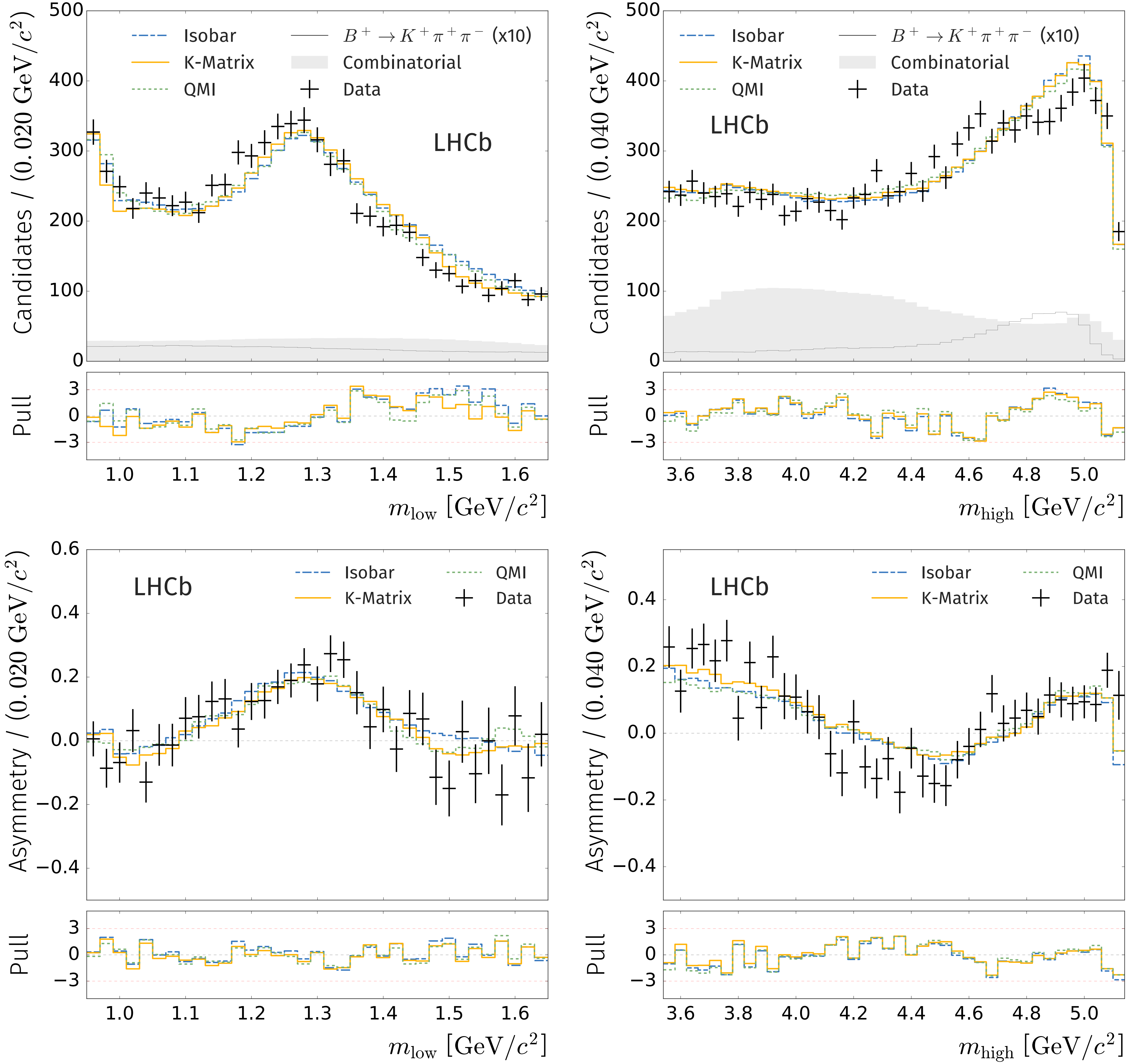
Isobar
K-Matrix
QMI
$B^+ \to K^+\pi^+\pi^-$ (x10)
Combinatorial
Data
LHCb
Candidates / (0.020 GeV/c^2)
Candidates / (0.040 GeV/c^2)
Asymmetry / (0.020 GeV/c^2)
Asymmetry / (0.040 GeV/c^2)
Pull
$m_{\rm low}$ [GeV/c^2]
$m_{\rm high}$ [GeV/c^2]

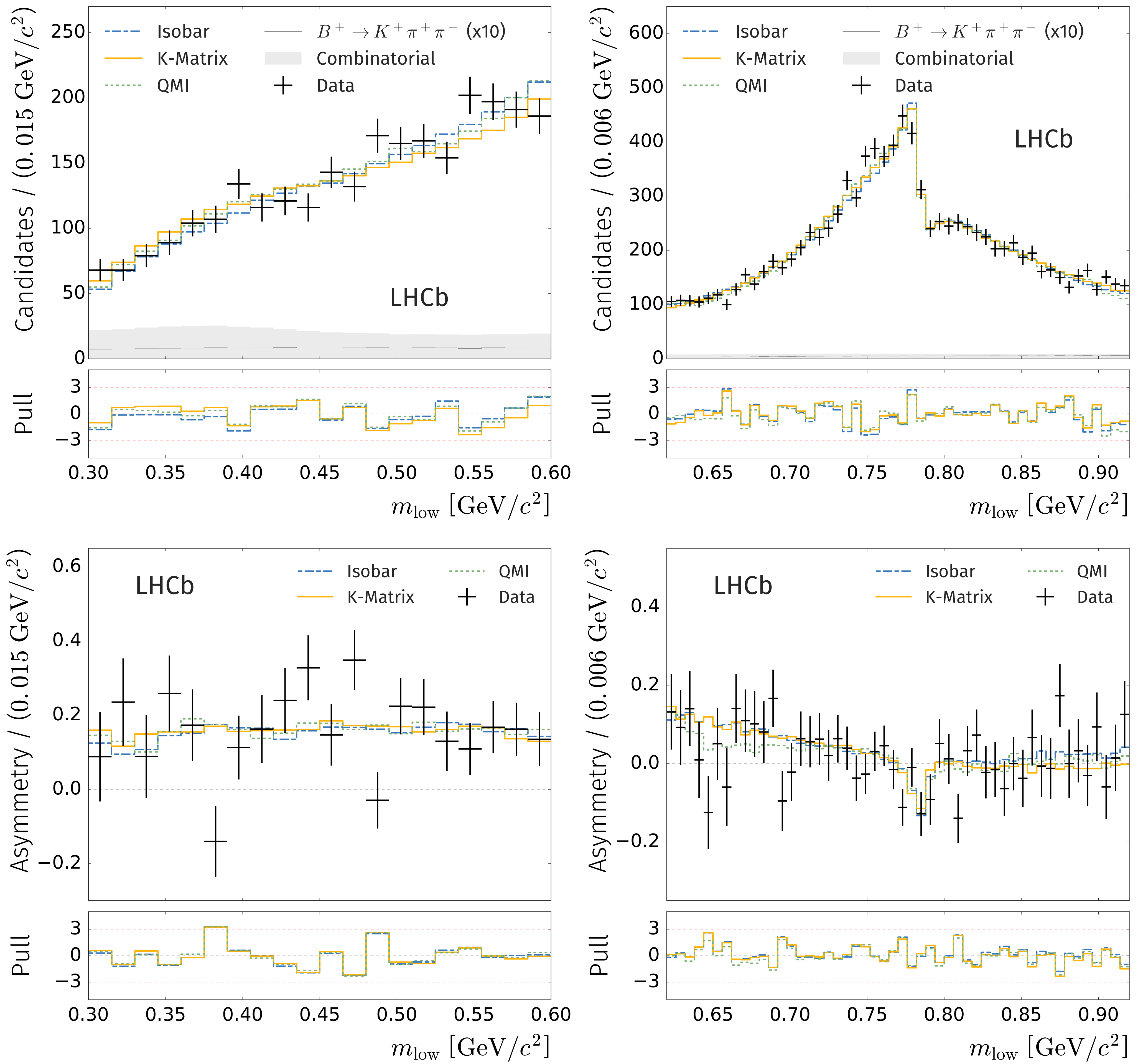
Isobar
K-Matrix
QMI
$B^+ \to K^+\pi^+\pi^-$ (x10)
Combinatorial
Data
LHCb
Candidates / (0.015 GeV/c^2)
Candidates / (0.006 GeV/c^2)
Asymmetry / (0.015 GeV/c^2)
Asymmetry / (0.006 GeV/c^2)
Pull
m_{low} [GeV/c^2]

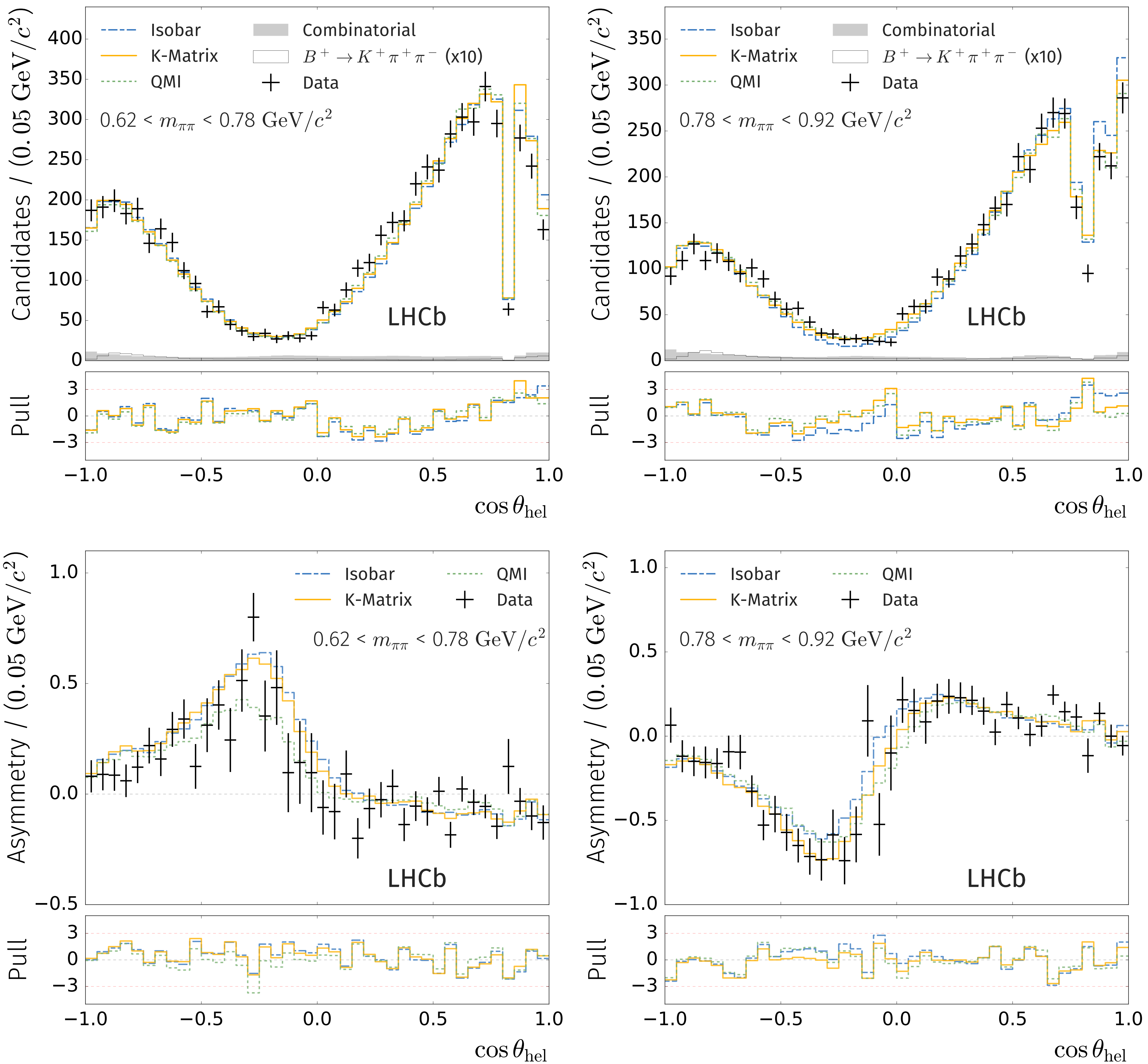

Isobar
K-Matrix
QMI
Combinatorial
$B^+ \to K^+\pi^+\pi^-$ (x10)
Data
$0.62 < m_{\pi\pi} < 0.78\ \mathrm{GeV}/c^2$
$0.78 < m_{\pi\pi} < 0.92\ \mathrm{GeV}/c^2$
LHCb
Candidates / (0.05 GeV/c^2)
Asymmetry / (0.05 GeV/c^2)
Pull
$\cos\theta_{\mathrm{hel}}$

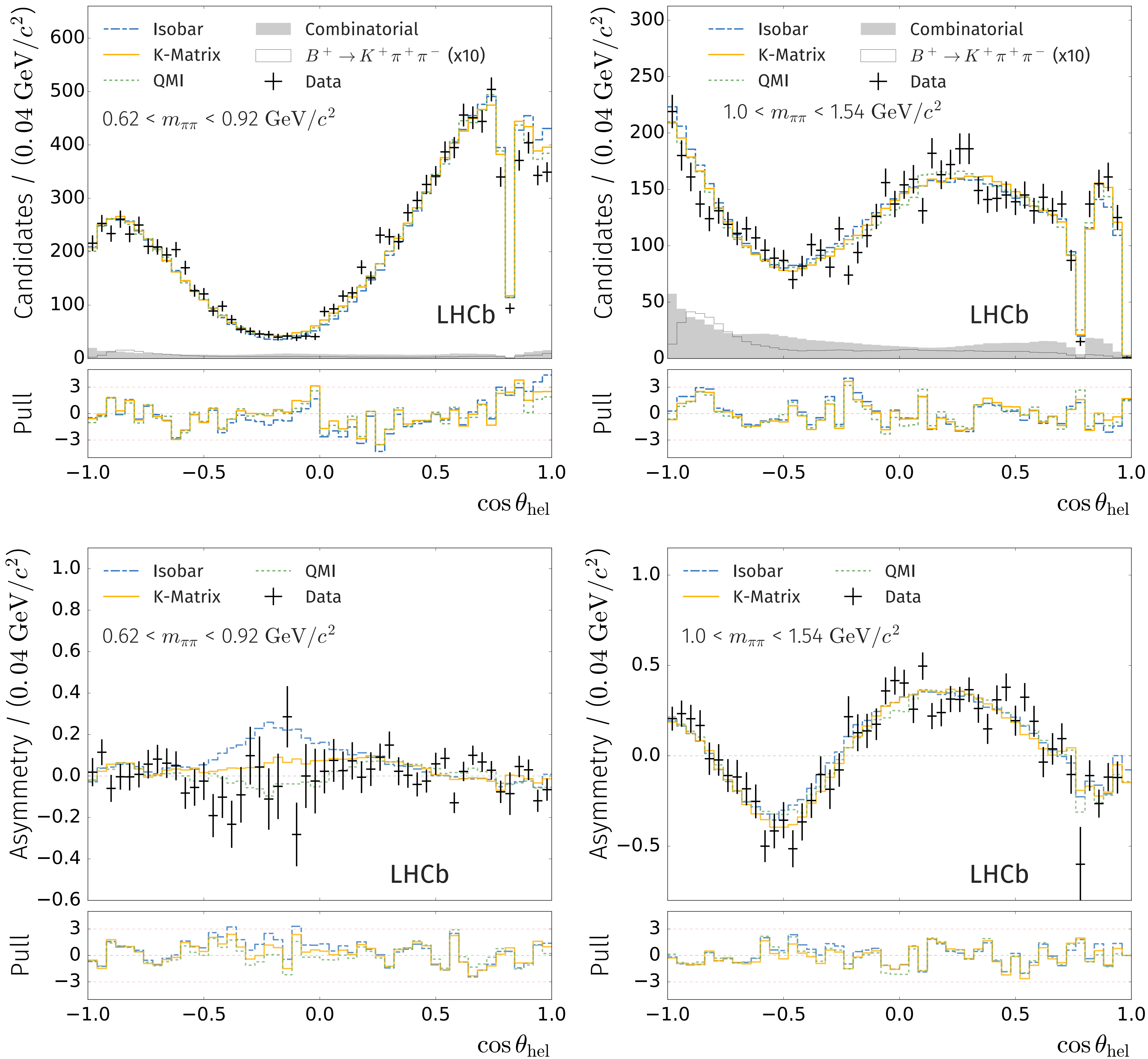
Isobar
K-Matrix
QMI
Combinatorial
$B^+ \to K^+\pi^+\pi^-$ (x10)
Data
$0.62 < m_{\pi\pi} < 0.92$ GeV$/c^2$
$1.0 < m_{\pi\pi} < 1.54$ GeV$/c^2$
LHCb
Candidates / (0.04 GeV$/c^2$)
Asymmetry / (0.04 GeV$/c^2$)
Pull
$\cos\theta_{\rm hel}$

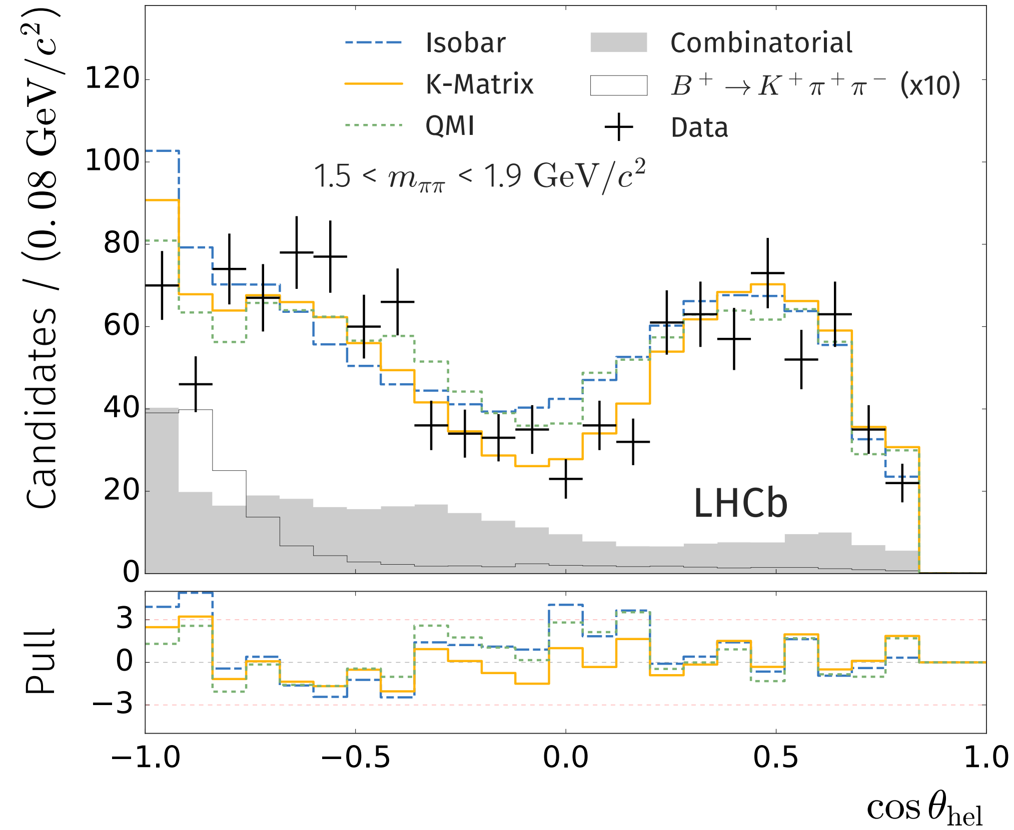

Isobar
K-Matrix
QMI
Combinatorial
$B^+ \to K^+\pi^+\pi^-$ (x10)
Data
1.5 < $m_{\pi\pi}$ < 1.9 GeV/c^2
LHCb
Candidates / (0.08 GeV/c^2)
Pull
$\cos\theta_{\rm hel}$

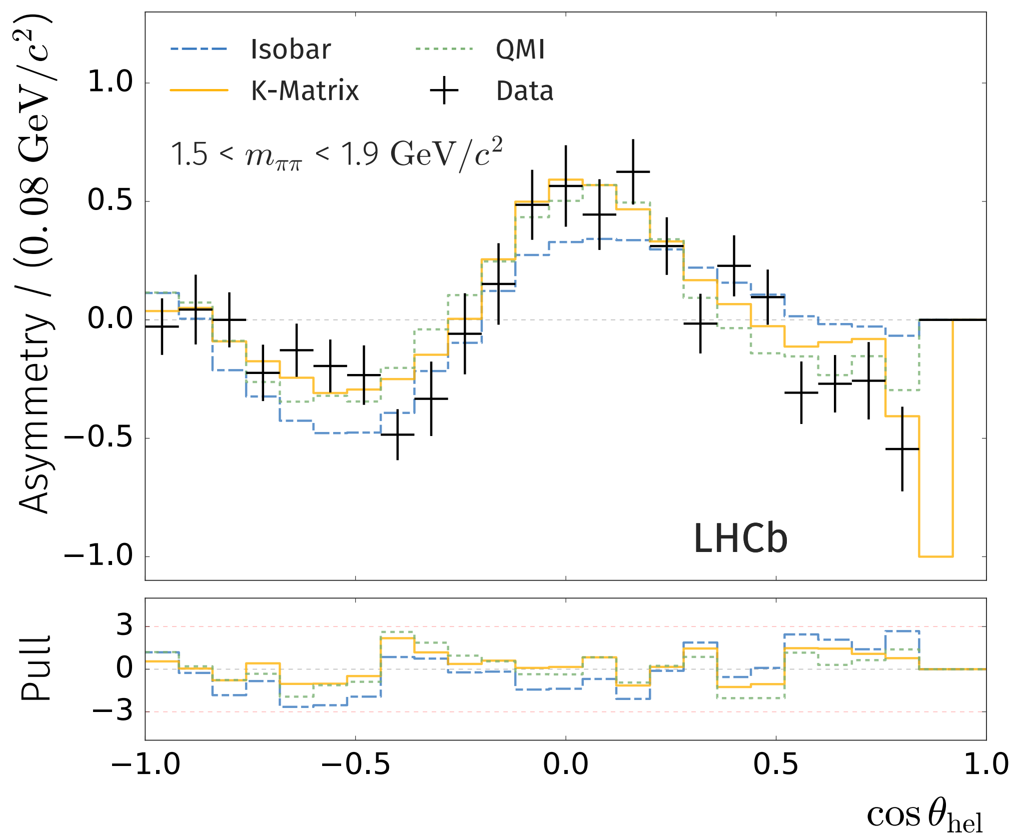

Isobar
K-Matrix
QMI
Data
1.5 < $m_{\pi\pi}$ < 1.9 GeV/c^2
LHCb
Asymmetry / (0.08 GeV/c^2)
Pull
$\cos\theta_{\rm hel}$

Search for CP and P violation in $\Lambda_b^0 \to p^+\pi^-\pi^+\pi^-$ decays

Table 2: Results obtained with different binning schemes; the p-value takes into account systematic effects and is reported for the CP and P conserving hypotheses.

Binning scheme	Dominant contribution	Hypothis	p-value
$[A]$ (in $\|\Phi\|$)	Entire sample	CP conserving	5.0×10^{-3}
		P conserving	3.5×10^{-7}
$[A_1]$ (in $\|\Phi\|$)	$\Lambda_b^0 \to pa_1^-$	CP conserving	4.7×10^{-2}
		P conserving	4.3×10^{-8}
$[A_2]$ (in $\|\Phi\|$)	$\Lambda_b^0 \to N^{*+}\pi^-$	CP conserving	3.4×10^{-3}
		P conserving	1.9×10^{-3}
$[B_1]$ (helicity angles)	$\Lambda_b^0 \to pa_1^-$	CP conserving	9.8×10^{-2}
		P conserving	1.8×10^{-5}
$[B_2]$ (helicity angles)	$\Lambda_b^0 \to N^{*+}\pi^-$	CP conserving	6.4×10^{-1}
		P conserving	6.4×10^{-2}

Search for CP and P violation in $\Lambda_b^0 \to p^+\pi^-\pi^+\pi^-$ decays

Table 3: p-values for the energy test.

δ	$1.6\ \mathrm{GeV}^2/c^4$	$2.7\ \mathrm{GeV}^2/c^4$	$13\ \mathrm{GeV}^2/c^4$
p-value (CP-conservation, P-even)	0.031	0.0027	0.013
p-value (CP-conservation, P-odd)	0.15	0.069	0.065
p-value (P-conservation)	1.3×10^{-7}	4.0×10^{-7}	0.16

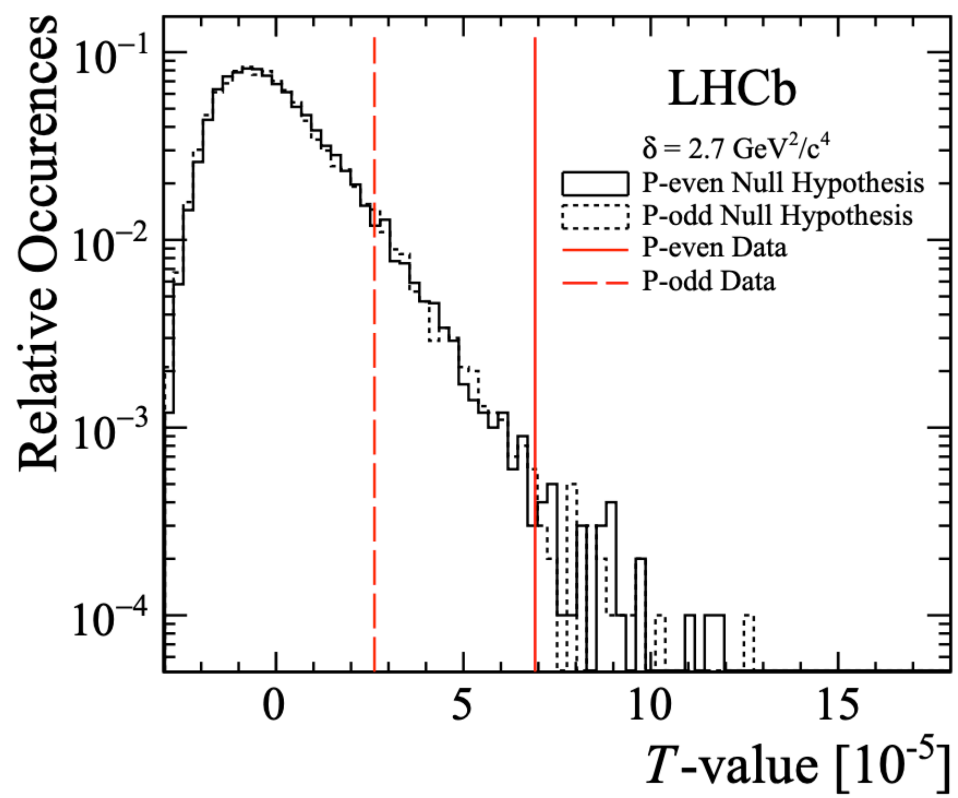

Figure 3: Distributions of T values under the null hypothesis obtained from permutations, using the energy test with $\delta = 2.7\,\mathrm{GeV}^2/c^4$ in the P-even and P-odd configurations when searching for CP violation. The values of T for real data are shown as red lines.

Search for CP and P violation in $\Lambda_b^0 \to p^+\pi^-\pi^+\pi^-$ decays

Table 4: Definition of the binning scheme [B]. This binning scheme is based on the helicity angles of the decay topology $\Lambda_b^0 \to (N^{*+} \to (\Delta^{++} \to p\pi^+)\,\pi^-)\,\pi^-$ where φ is the azimuthal angle of the proton in the Δ^{++} rest frame and $\theta_{\Delta^{++}}$ (θ_p) is the polar angle of the Δ^{++} (p) in the N^{*+} (Δ^{++}) rest frame.

Bin number	Polar angles	Azimuthal angles
1	$\theta_p \in [0, \pi/4]$ & $\theta_{\Delta^{++}} \in [0, \pi/4]$ $\theta_p \in [\pi/2, 3\pi/4]$ & $\theta_{\Delta^{++}} \in [\pi/2, 3\pi/4]$	$\lvert\varphi\rvert \in [0, \pi/2]$
2	$\theta_p \in [0, \pi/4]$ & $\theta_{\Delta^{++}} \in [\pi/4, \pi/2]$ $\theta_p \in [\pi/2, 3\pi/4]$ & $\theta_{\Delta^{++}} \in [3\pi/4, \pi]$	$\lvert\varphi\rvert \in [0, \pi/2]$
3	$\theta_p \in [0, \pi/4]$ & $\theta_{\Delta^{++}} \in [\pi/2, 3\pi/4]$ $\theta_p \in [\pi/2, 3\pi/4]$ & $\theta_{\Delta^{++}} \in [0, \pi/4]$	$\lvert\varphi\rvert \in [0, \pi/2]$
4	$\theta_p \in [0, \pi/4]$ & $\theta_{\Delta^{++}} \in [3\pi/4, \pi]$ $\theta_p \in [\pi/2, 3\pi/4]$ & $\theta_{\Delta^{++}} \in [\pi/4, \pi/2]$	$\lvert\varphi\rvert \in [0, \pi/2]$
5	$\theta_p \in [\pi/4, \pi/2]$ & $\theta_{\Delta^{++}} \in [0, \pi/4]$ $\theta_p \in [3\pi/4, \pi]$ & $\theta_{\Delta^{++}} \in [\pi/2, 3\pi/4]$	$\lvert\varphi\rvert \in [0, \pi/2]$
6	$\theta_p \in [\pi/4, \pi/2]$ & $\theta_{\Delta^{++}} \in [\pi/4, \pi/2]$ $\theta_p \in [3\pi/4, \pi]$ & $\theta_{\Delta^{++}} \in [3\pi/4, \pi]$	$\lvert\varphi\rvert \in [0, \pi/2]$
7	$\theta_p \in [\pi/4, \pi/2]$ & $\theta_{\Delta^{++}} \in [\pi/2, 3\pi/4]$ $\theta_p \in [3\pi/4, \pi]$ & $\theta_{\Delta^{++}} \in [0, \pi/4]$	$\lvert\varphi\rvert \in [0, \pi/2]$
8	$\theta_p \in [\pi/4, \pi/2]$ & $\theta_{\Delta^{++}} \in [3\pi/4, \pi]$ $\theta_p \in [3\pi/4, \pi]$ & $\theta_{\Delta^{++}} \in [\pi/4, \pi/2]$	$\lvert\varphi\rvert \in [0, \pi/2]$

Search for CP and P violation in $\Lambda_b^0 \to p^+\pi^-\pi^+\pi^-$ decays

(Continued)

9	$\theta_p \in [0, \pi/4]$ & $\theta_{\Delta^{++}} \in [0, \pi/4]$ $\theta_p \in [\pi/2, 3\pi/4]$ & $\theta_{\Delta^{++}} \in [\pi/2, 3\pi/4]$	$\lvert\varphi\rvert \in [\pi/2, \pi]$
10	$\theta_p \in [0, \pi/4]$ & $\theta_{\Delta^{++}} \in [\pi/4, \pi/2]$ $\theta_p \in [\pi/2, 3\pi/4]$ & $\theta_{\Delta^{++}} \in [3\pi/4, \pi]$	$\lvert\varphi\rvert \in [\pi/2, \pi]$
11	$\theta_p \in [0, \pi/4]$ & $\theta_{\Delta^{++}} \in [\pi/2, 3\pi/4]$ $\theta_p \in [\pi/2, 3\pi/4]$ & $\theta_{\Delta^{++}} \in [0, \pi/4]$	$\lvert\varphi\rvert \in [\pi/2, \pi]$
12	$\theta_p \in [0, \pi/4]$ & $\theta_{\Delta^{++}} \in [3\pi/4, \pi]$ $\theta_p \in [\pi/2, 3\pi/4]$ & $\theta_{\Delta^{++}} \in [\pi/4, \pi/2]$	$\lvert\varphi\rvert \in [\pi/2, \pi]$
13	$\theta_p \in [\pi/4, \pi/2]$ & $\theta_{\Delta^{++}} \in [0, \pi/4]$ $\theta_p \in [3\pi/4, \pi]$ & $\theta_{\Delta^{++}} \in [\pi/2, 3\pi/4]$	$\lvert\varphi\rvert \in [\pi/2, \pi]$
14	$\theta_p \in [\pi/4, \pi/2]$ & $\theta_{\Delta^{++}} \in [\pi/4, \pi/2]$ $\theta_p \in [3\pi/4, \pi]$ & $\theta_{\Delta^{++}} \in [3\pi/4, \pi]$	$\lvert\varphi\rvert \in [\pi/2, \pi]$
15	$\theta_p \in [\pi/4, \pi/2]$ & $\theta_{\Delta^{++}} \in [\pi/2, 3\pi/4]$ $\theta_p \in [3\pi/4, \pi]$ & $\theta_{\Delta^{++}} \in [0, \pi/4]$	$\lvert\varphi\rvert \in [\pi/2, \pi]$
16	$\theta_p \in [\pi/4, \pi/2]$ & $\theta_{\Delta^{++}} \in [3\pi/4, \pi]$ $\theta_p \in [3\pi/4, \pi]$ & $\theta_{\Delta^{++}} \in [\pi/4, \pi/2]$	$\lvert\varphi\rvert \in [\pi/2, \pi]$

$B^0_{(s)} \to \phi\phi$

LHCB-PAPER-2019-019 (arXiv:1907.10003)

5fb^{-1} of data (2011 - 2016)

Time dependent, tagged, angular analysis:
Separate different helicity components,
for B^0_s and $\overline{B}^0_s$

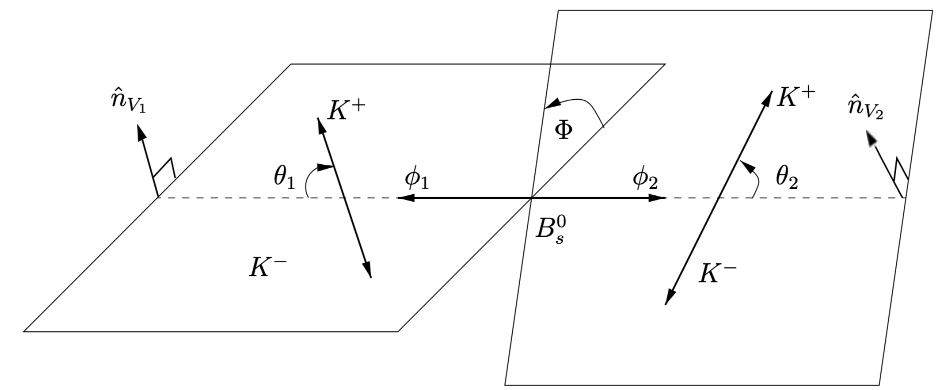

Select candidates in window $\pm 25\ \mathrm{MeV}/c^2$ of the known ϕ mass (account for small amount of $f_0(980)$ in the model)

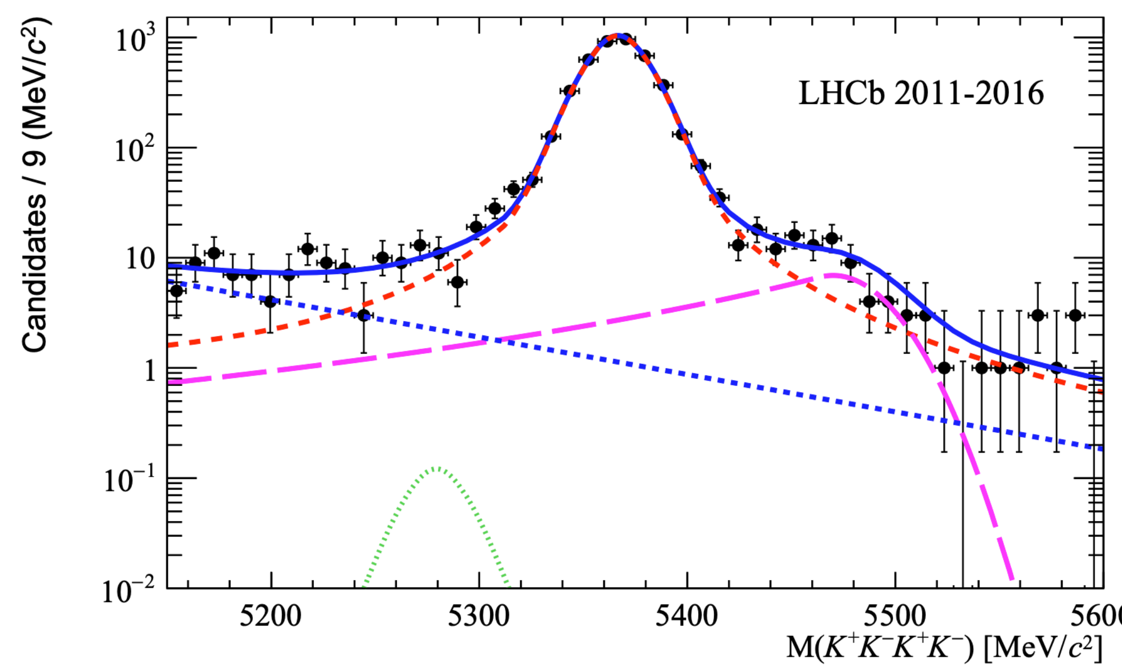

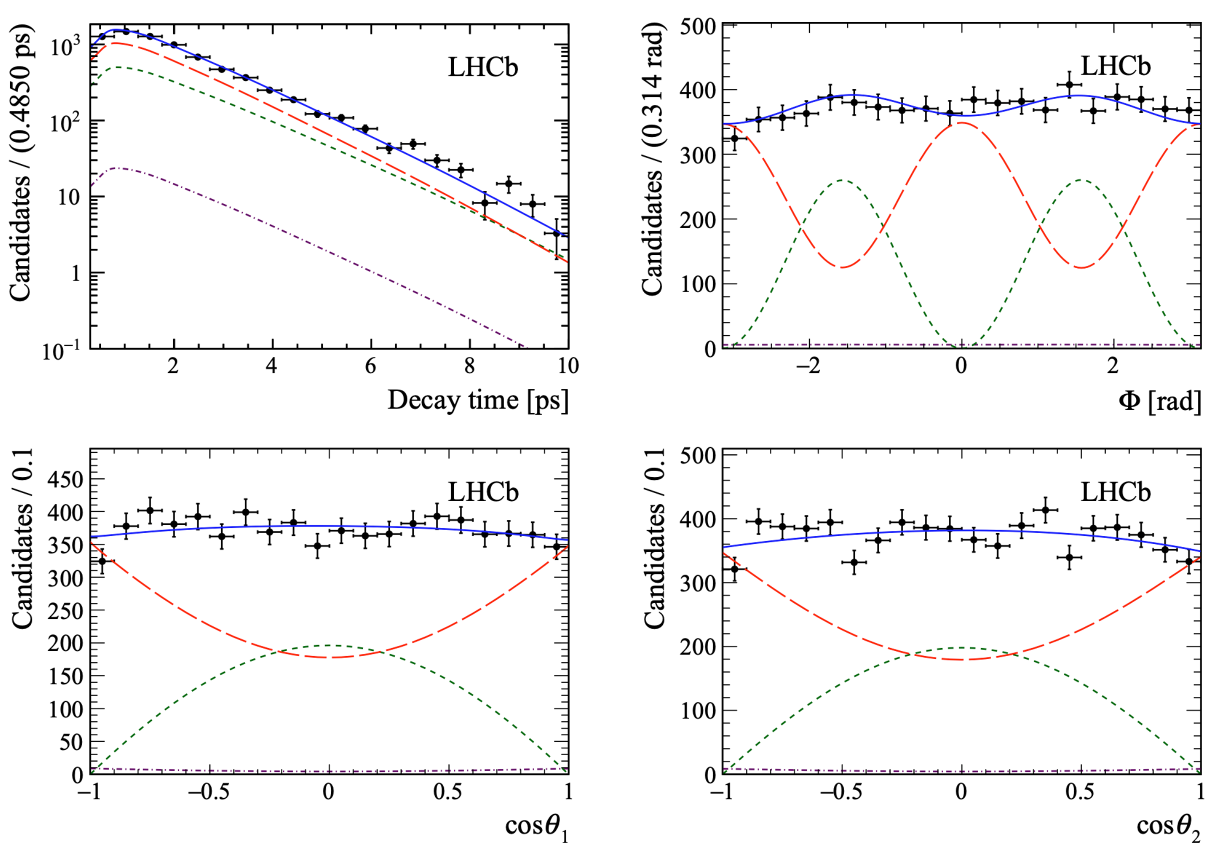

Tag initial flavour with ‘opposite side’, and ‘same side’ kaon flavour taggers, with a tagging power ($\epsilon\mathcal{D}^2$) of around **5.7%**

$B^0_{(s)} \to \phi\phi$

LHCB-PAPER-2019-019 (arXiv:1907.10003)

Measurement of CP violating phase:

$$\phi_s^{s\bar{s}s} = -0.073 \pm 0.115 \pm 0.027$$

consistent with the Standard Model expectation (upper limit of $|\phi_s^{s\bar{s}s}| < 0.02$ from QCDf), previous measurements, and the most precise single-experiment result to-date

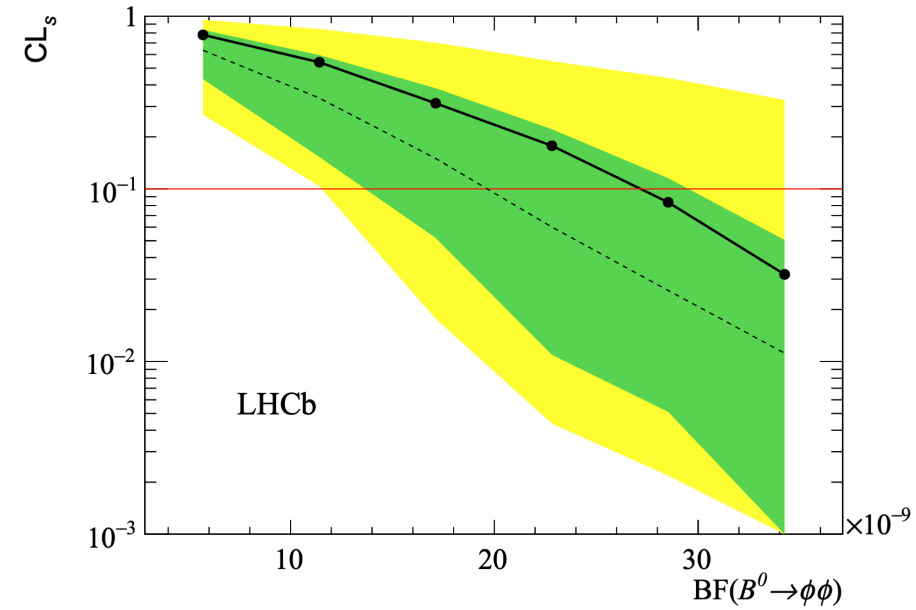

Limit on $B^0 \to \phi\phi$

(Suppressed by OZI)

Measurement of CP violating triple-product asymmetries, consistent with CP conservation (combination of Run 1 and 2):

$$A_U = -0.003 \pm 0.011\,(\text{stat}) \pm 0.004\,(\text{syst}),$$
$$A_V = -0.014 \pm 0.011\,(\text{stat}) \pm 0.004\,(\text{syst}),$$

Direct CP violation parameter also consistent with CP conservation:

$$|\lambda| = 0.99 \pm 0.05\,(\text{stat}) \pm 0.01\,(\text{syst})$$

$B^0_{(s)} \to \phi\phi$

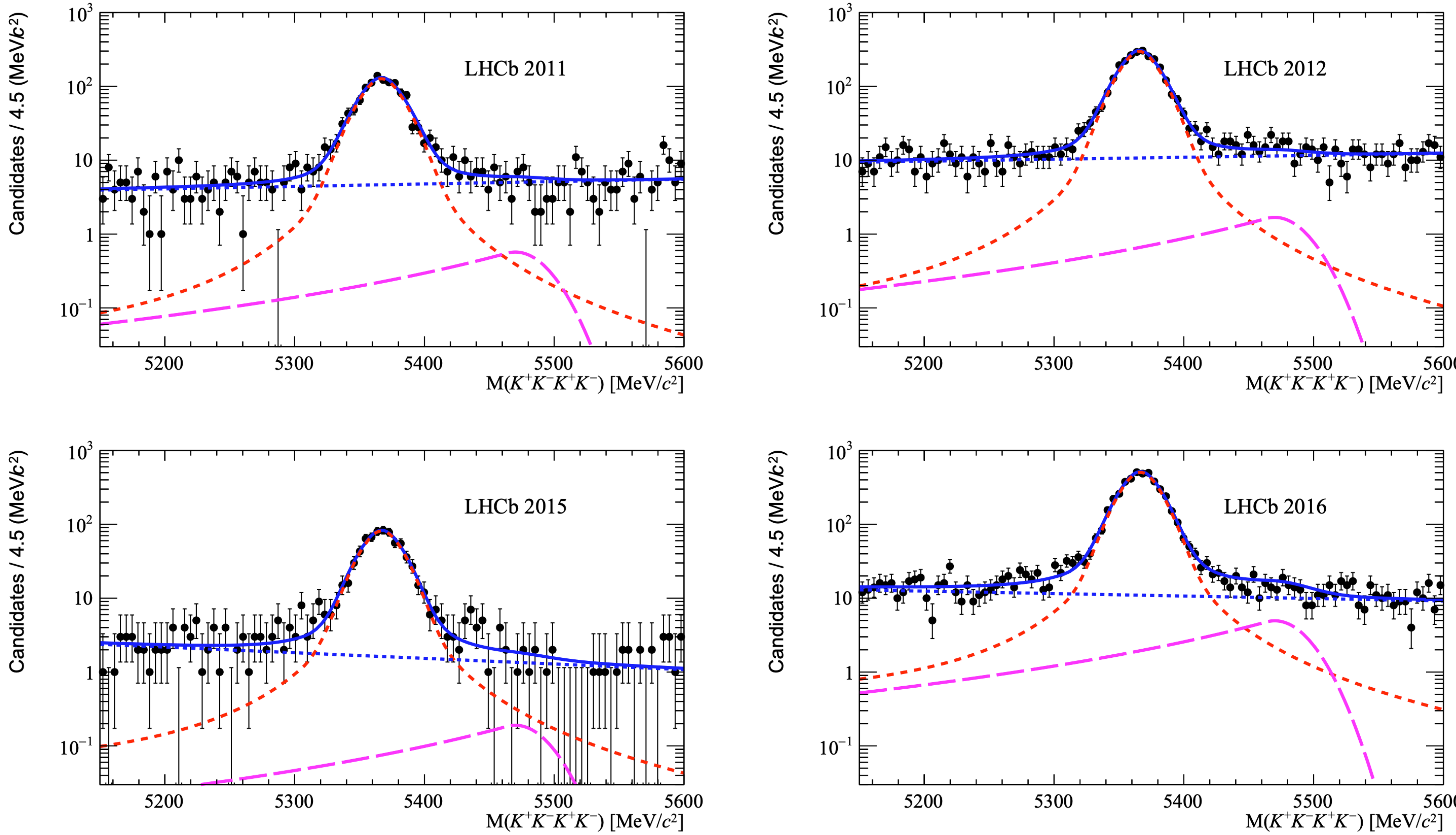

$B^0_{(s)} \to \phi\phi$ future prospects

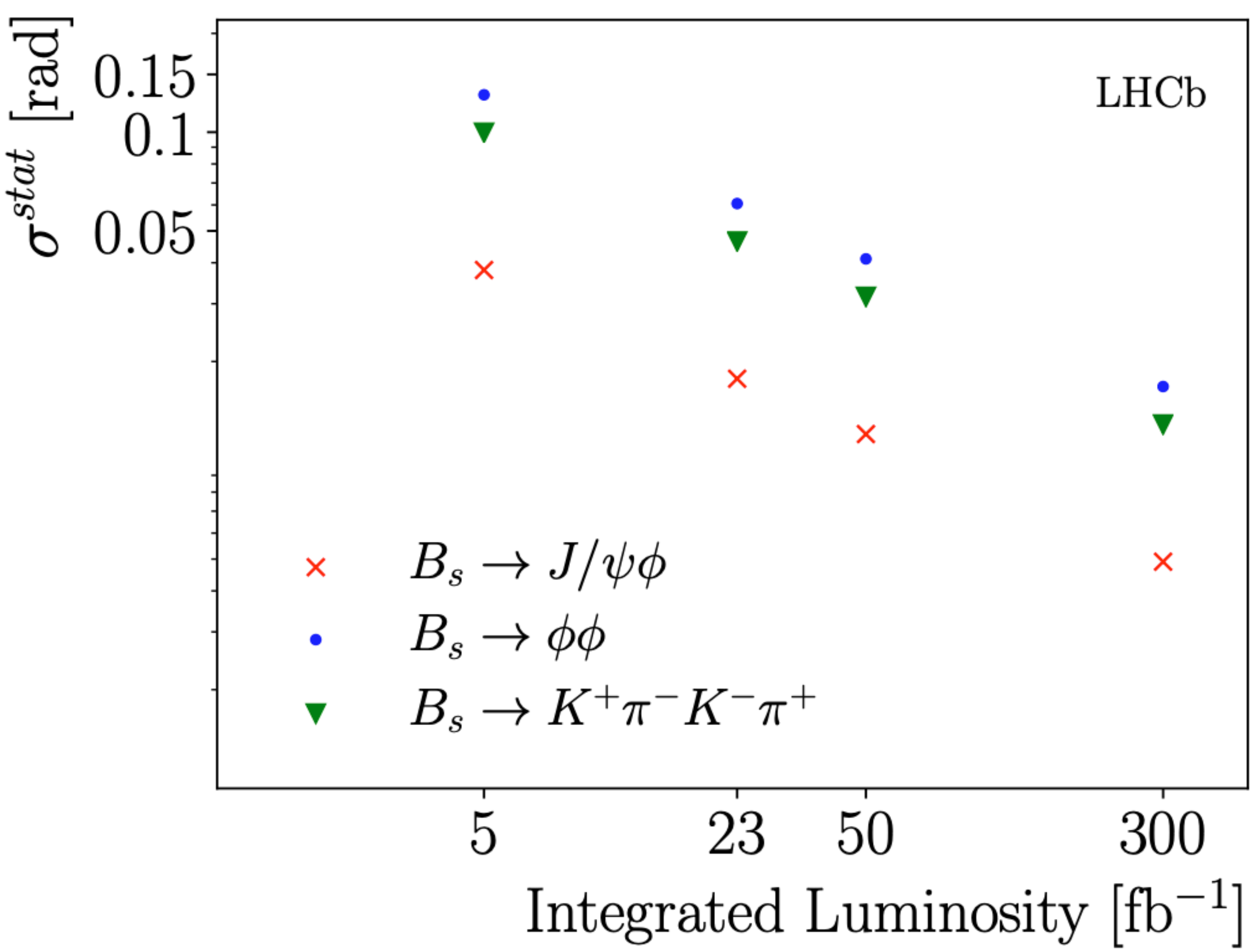

$B^0_{(s)} \to \phi\phi$ polarisation dependent results

$$\begin{aligned}
\phi_{s,\parallel} &= 0.014 \pm 0.055\,(\text{stat}) \pm 0.011\,(\text{syst})\ \text{rad},\\
\phi_{s,\perp} &= 0.044 \pm 0.059\,(\text{stat}) \pm 0.019\,(\text{syst})\ \text{rad}.
\end{aligned}$$

$$\begin{aligned}
|A_0|^2 &= 0.381 \pm 0.007\,(\text{stat}) \pm 0.012\,(\text{syst}),\\
|A_\perp|^2 &= 0.290 \pm 0.008\,(\text{stat}) \pm 0.007\,(\text{syst}),\\
\delta_\perp &= 2.818 \pm 0.178\,(\text{stat}) \pm 0.073\,(\text{syst})\ \text{rad},\\
\delta_\parallel &= 2.559 \pm 0.045\,(\text{stat}) \pm 0.033\,(\text{syst})\ \text{rad}.
\end{aligned}$$